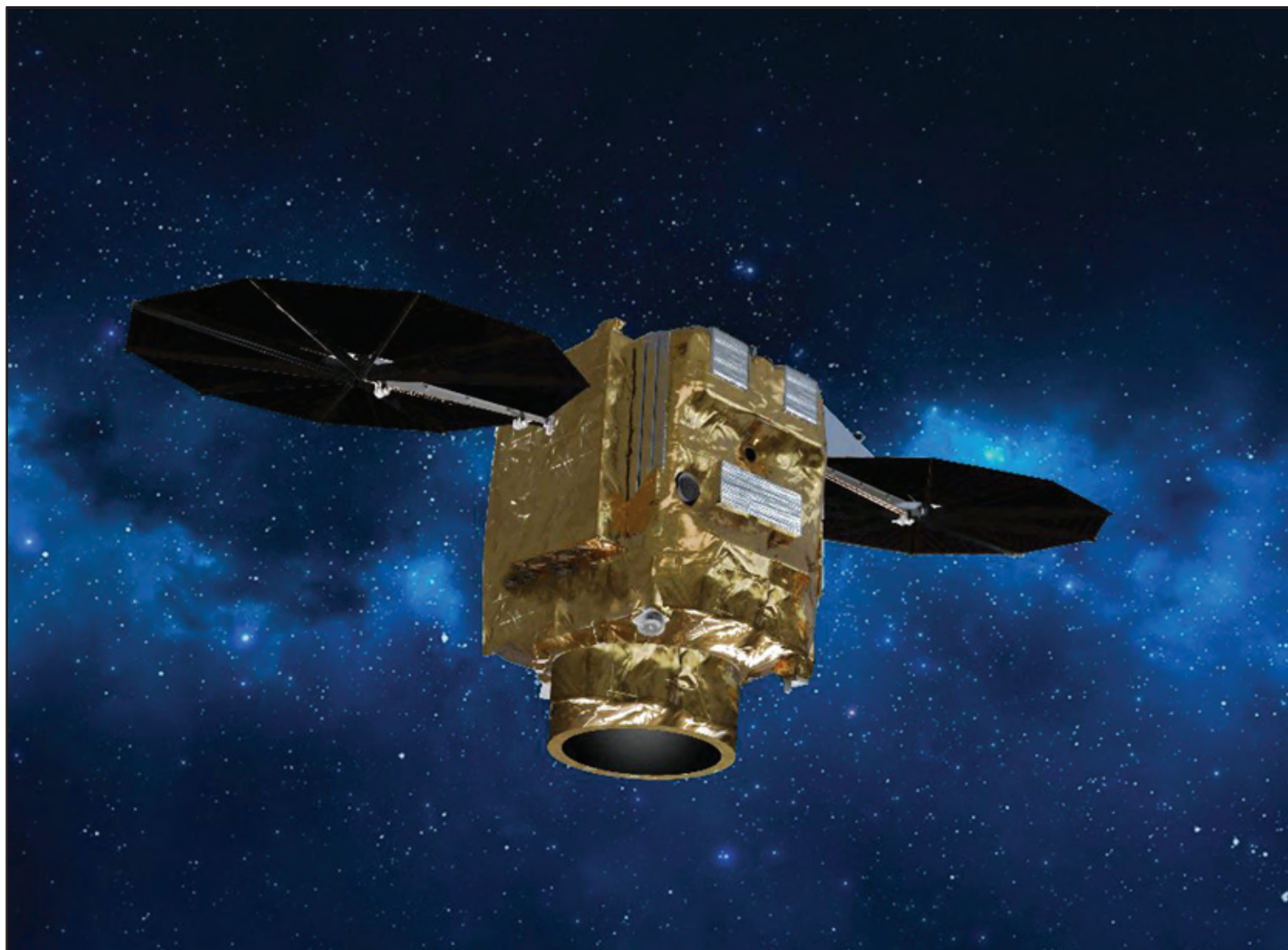


System Characterization Report on the Pléiades Neo Imager

Chapter P of
System Characterization of Earth Observation Sensors



Open-File Report 2021–1030–P
Version 1.1, April 2024

U.S. Department of the Interior
U.S. Geological Survey

Cover. Artistic rendering of Pléiades Neo in orbit. Image courtesy of Airbus Defence and Space; used with permission.

System Characterization Report on the Pléiades Neo Imager

By Simon J. Cantrell,¹ Aparajithan Sampath,¹ James C. Vrabel,² Paul Bresnahan,¹ Cody Anderson,³ Minsu Kim,¹ and Seonkyung Park¹

Chapter P of System Characterization of Earth Observation Sensors

Compiled by Shankar N. Ramaseri Chandra¹

¹KBR, Inc., under contract to the
U.S. Geological Survey.

²Imaging Technology Consultants, Inc.,
under contract to the U.S. Geological Survey.

³U.S. Geological Survey.

Open-File Report 2021–1030–P
Version 1.1, April 2024

U.S. Department of the Interior
U.S. Geological Survey

U.S. Geological Survey, Reston, Virginia: 2023

First release: 2023

Revised: April 2024 (ver. 1.1)

For more information on the USGS—the Federal source for science about the Earth, its natural and living resources, natural hazards, and the environment—visit <https://www.usgs.gov> or call 1–888–392–8545.

For an overview of USGS information products, including maps, imagery, and publications, visit <https://store.usgs.gov/> or contact the store at 1–888–275–8747.

Any use of trade, firm, or product names is for descriptive purposes only and does not imply endorsement by the U.S. Government.

Although this information product, for the most part, is in the public domain, it also may contain copyrighted materials as noted in the text. Permission to reproduce copyrighted items must be secured from the copyright owner.

Suggested citation:

Cantrell, S.J., Sampath, A., Vrabel, J.C., Bresnahan, P., Anderson, C., Kim, M., and Park, S., 2023, System characterization report on the Pléiades Neo Imager (ver. 1.1, April 2024), chap. P of Ramaseri Chandra, S.N., comp., System characterization of Earth observation sensors: U.S. Geological Survey Open-File Report 2021–1030, 52 p., <https://doi.org/10.3133/ofr20211030P>.

ISSN 2331-1258 (online)

Contents

Executive Summary	1
Introduction.....	1
Purpose and Scope	2
System Description.....	2
Satellite and Operational Details	2
Sensor Information	2
Procedures.....	4
Measurements	4
Analysis	6
Geometric Performance	6
Interior (Band to Band)	6
Exterior (Geometric Location Accuracy)	31
Radiometric Performance	46
Spatial Performance	48
Summary and Conclusions.....	51
Selected References.....	51
Appendix 1. Explanation of Ground Control Points Method and Metadata.....	52

Figures

1. Graph showing Pléiades Neo visible and near-infrared relative spectral response	4
2. Band 3 to band 4 geometric error map of Boulder, Colorado.....	7
3. Band 3 to band 4 geometric error histogram for Boulder, Colorado	8
4. Band 3 to band 4 geometric error plot for Boulder, Colorado	8
5. Band 4 to band 5 geometric error map of Boulder, Colorado.....	9
6. Band 4 to band 5 geometric error histogram for Boulder, Colorado	10
7. Band 4 to band 5 geometric error plot for Boulder, Colorado	10
8. Band 6 to band 7 geometric error map of Boulder, Colorado.....	11
9. Band 6 to band 7 geometric error histogram for Boulder, Colorado	12
10. Band 6 to band 7 geometric error plot for Boulder, Colorado	12
11. Band 3 to band 4 geometric error map of Baotou, Inner Mongolia, China	13
12. Band 3 to band 4 geometric error histogram for Baotou, Inner Mongolia, China	14
13. Band 3 to band 4 geometric error plot for Baotou, Inner Mongolia, China	14
14. Band 4 to band 5 geometric error map for Baotou, Inner Mongolia, China	15
15. Band 4 to band 5 geometric error histogram for Baotou, Inner Mongolia, China	16
16. Band 4 to band 5 geometric error plot for Baotou, Inner Mongolia, China	16
17. Band 6 to band 7 geometric error map of Baotou, Inner Mongolia, China	17
18. Band 6 to band 7 geometric error histogram for Baotou, Inner Mongolia, China	18
19. Band 6 to band 7 geometric error plot for Baotou, Inner Mongolia, China	18
20. Band 3 to band 4 geometric error map for Sioux Falls, South Dakota.....	19
21. Band 3 to band 4 geometric error histogram of Sioux Falls, South Dakota	20
22. Band 3 to band 4 geometric error plot for Sioux Falls, South Dakota.....	20
23. Band 4 to band 5 geometric error map for Sioux Falls, South Dakota.....	21

24.	Band 4 to band 5 geometric error histogram for Sioux Falls, South Dakota	22
25.	Band 4 to band 5 geometric error plot for Sioux Falls, South Dakota.....	22
26.	Band 6 to band 7 geometric error map for Sioux Falls, South Dakota.....	23
27.	Band 6 to band 7 geometric error histogram for Sioux Falls, South Dakota	24
28.	Band 6 to band 7 geometric error plot for Sioux Falls, South Dakota.....	24
29.	Band 3 to band 4 geometric error map for Fort Lupton, Colorado.....	25
30.	Band 3 to band 4 geometric error histogram of Fort Lupton, Colorado.....	26
31.	Band 3 to band 4 geometric error plot for Fort Lupton, Colorado.....	26
32.	Band 4 to band 5 geometric error map for Fort Lupton, Colorado.....	27
33.	Band 4 to band 5 geometric error histogram for Fort Lupton, Colorado	28
34.	Band 4 to band 5 geometric error plot for Fort Lupton, Colorado.....	28
35.	Band 6 to band 7 geometric error map for Fort Lupton, Colorado.....	29
36.	Band 6 to band 7 geometric error histogram for Fort Lupton, Colorado	30
37.	Band 6 to band 7 geometric error plot for Fort Lupton, Colorado.....	30
38.	Map showing relative geometric error comparison for Sentinel-2 and Pléiades Neo for the near-infrared band, Sioux Falls, South Dakota.....	33
39.	Relative geometric easting and northing error histogram comparison for Sentinel-2 and Pléiades Neo for the near-infrared band, Sioux Falls, South Dakota	34
40.	Relative geometric easting and northing error plot comparison for Sentinel-2 and Pléiades Neo for the near-infrared band, Sioux Falls, South Dakota	34
41.	Map showing relative geometric error comparison for Sentinel-2 and Pléiades Neo for the near-infrared band, Fort Lupton, Colorado.....	35
42.	Relative geometric easting and northing error histogram comparison for Sentinel-2 and Pléiades Neo for the near-infrared band, Fort Lupton, Colorado	36
43.	Relative geometric easting and northing error plot comparison for Sentinel-2 and Pléiades Neo for the near-infrared band, Fort Lupton, Colorado	36
44.	Relative geometric error comparison for Sentinel-2 and Pléiades Neo orthorectified image for the near-infrared band, Baotou, Inner Mongolia, China	37
45.	Relative geometric easting and northing error histogram comparison for Sentinel-2 and Pléiades Neo orthorectified image for the near-infrared band, Baotou, Inner Mongolia, China.....	38
46.	Relative geometric easting and northing error plot comparison for Sentinel-2 and Pléiades Neo orthorectified image for the near-infrared band, Baotou, Inner Mongolia, China.....	38
47.	Relative geometric error comparison for Sentinel-2 and Pléiades Neo orthorectified image for the near-infrared band, Fort Lupton, Colorado.....	39
48.	Relative geometric easting and northing error histogram comparison for Sentinel-2 and Pléiades Neo orthorectified image for the near-infrared band, Fort Lupton, Colorado.....	39
49.	Relative geometric easting and northing error plot comparison for Sentinel-2 and Pléiades Neo orthorectified image for the near-infrared band, Fort Lupton, Colorado	43
50.	Relative geometric error comparison for Sentinel-2 and Pléiades Neo orthorectified image for the near-infrared band, Sioux Falls, South Dakota.....	43
51.	Relative geometric easting and northing error histogram comparison for Sentinel-2 and Pléiades Neo orthorectified image for the near-infrared band, Sioux Falls, South Dakota	44

52.	Relative geometric easting and northing error plot comparison for Sentinel-2 and Pléiades Neo orthorectified image for the near-infrared band, Sioux Falls, South Dakota	44
53.	Pléiades Neo horizontal geolocation accuracy error plot for primary panchromatic and red, green, and blue and orthorectified panchromatic; red, green, and blue; and near-infrared, red edge, and deep blue band scenes	45
54.	Graphs showing Top of Atmosphere reflectance comparison for Pléiades Neo and Sentinel-2 for blue, green, red, and near-infrared bands for Fort Lupton, Colorado, on October 20, 2021	47
55.	Pléiades Neo image of calibration site at Baotou, Inner Mongolia, China	48
56.	Image showing band 1, panchromatic, raw edge transect selected within the region of interest at Baotou, Inner Mongolia, China	49
57.	Graphs showing band 1, panchromatic, raw edge transect, edge spread function, line spread function, and modulation transfer function at Baotou, Inner Mongolia, China	50

Tables

1.	Satellite and operational details for Pléiades Neo	3
2.	Imaging sensor details for Pléiades Neo	3
3.	U.S. Geological Survey measurement results	5
4.	Band-to-band registration error	6
5.	Geometric error relative to Sentinel-2	32
6.	Geometric error relative to Sentinel-2	32
7.	Geometric error of Pléiades Neo-4 primary panchromatic bands relative to ground-surveyed control points	40
8.	Geometric error of Pléiades Neo-4 primary red, green, and blue bands relative to ground-surveyed control points	40
9.	Geometric error of Pléiades Neo-4 orthorectified panchromatic bands relative to ground-surveyed control points	41
10.	Geometric error of Pléiades Neo-4 orthorectified red, green, and blue bands relative to ground-surveyed control points	41
11.	Geometric error of Pléiades Neo-4 orthorectified near-infrared, red edge, and deep blue bands relative to ground-surveyed control points	42
12.	Top of Atmosphere reflectance comparison of Pléiades Neo images against Sentinel-2 images	46
13.	Spatial performance of Pléiades Neo	48

Conversion Factors

International System of Units to U.S. customary units

Multiply	By	To obtain
Length		
centimeter (cm)	0.3937	inch (in.)
meter (m)	3.281	foot (ft)
meter (m)	1.094	yard (yd)
kilometer (km)	0.6214	mile (mi)

Abbreviations

ECCOE	Earth Resources Observation and Science Cal/Val Center of Excellence
GCP	ground control point
GSD	ground sample distance
JACIE	Joint Agency Commercial Imagery Evaluation
NED	near infrared, red edge, and deep blue
RGB	red, green, and blue
USGS	U.S. Geological Survey
VNIR	visible and near infrared

System Characterization Report on the Pléiades Neo Imager

By Simon J. Cantrell,¹ Aparajithan Sampath,¹ James C. Vrabel,² Paul Bresnahan,¹ Cody Anderson,³ Minsu Kim,¹ and Seonkyung Park¹

Executive Summary

This report addresses system characterization of the Pléiades Neo satellite and is part of a series of system characterization reports produced and delivered by the U.S. Geological Survey Earth Resources Observation and Science Cal/Val Center of Excellence. These reports present and detail the methodology and procedures for characterization; present technical and operational information about the specific sensing system being evaluated; and provide a summary of test measurements, data retention practices, data analysis results, and conclusions.

Pléiades Neo is a constellation of four identical very-high-resolution optical satellites operated by Airbus Defence and Space. The first two satellites, Pléiades Neo-3 and -4, were launched in April and August 2021, respectively. The next two satellites, launched in December 2022, did not reach orbit because of Vega-C launch vehicle failure. Pléiades Neo provides several technical improvements to previous Pléiades-HR satellites, including the addition of coastal aerosol (deep blue) and red edge spectral bands, with improved ground sample distance and swath. The Pléiades Neo satellites were designed and built by Airbus Defence and Space with the high-resolution, multispectral imager for Earth imaging and use the S950 optical satellite bus. The high-resolution sensor on Pléiades Neo collects Earth data in the visible and near-infrared region with six bands and a panchromatic band. The satellites can operate off nadir to achieve a revisit of less than 1 day. More information on Pléiades Neo satellites and sensors is available in the “Land Remote Sensing Satellites Online Compendium” (<https://calval.cr.usgs.gov/apps/compendium#>) and from the manufacturer (<https://www.intelligence-airbusds.com/imagery/constellation/pleiades-Neo/>).

The Earth Resources Observation and Science Cal/Val Center of Excellence system characterization team completed data analyses to characterize the geometric (interior and

exterior), radiometric, and spatial performances. Results of these analyses indicate that Pléiades Neo has an interior geometric performance in the range of 0.01 meter (m; 0.008 pixel) to -0.017 m (-0.014 pixel) in band-to-band registration; an exterior geometric performance in the range of -7.015 m (-0.702 pixel) to 3.846 m (0.385 pixel) offset in comparison to Sentinel-2 using ground control points of 2.2 to 7.2 m (95-percent circular error); a radiometric performance in the range of -0.070 (minimum) to -0.053 (maximum) in offset and 1.107 (minimum) to 1.202 (maximum) in slope; and a spatial performance in the range of 1.002 to 1.226 pixels at full width at half maximum with a modulation transfer function at a Nyquist frequency in the range of 0.22 to 0.34 (bands 2–7).

Introduction

The imaging sensor onboard Pléiades Neo was built by Airbus Defence and Space. The Pléiades Neo imager provides the three visible and near-infrared (VNIR) bands similar to Pléiades-HR and adds two visible bands, for deep blue (coastal aerosol) and red edge. The ground sample distance (GSD) is improved to 30 centimeters for panchromatic data and to 1.2 meters (m) in VNIR. The swath is improved to 14 kilometers, and the revisit is less than 1 day across the constellation. Data are available to customers through the Airbus Defence and Space commercial portal.

The data analysis results provided in this report have been derived from industry approved Joint Agency Commercial Imagery Evaluation (JACIE) processes and procedures. JACIE was formed to leverage resources from several Federal agencies for the characterization of remote sensing data and to share those results across the remote sensing community. More information about JACIE is available at https://www.usgs.gov/calval/jacie?qt-science_support_page_related_con=3#qt-science_support_page_related_con.

¹KBR, Inc., under contract to the U.S. Geological Survey.

²Imaging Technology Consultants, Inc., under contract to the U.S. Geological Survey.

³U.S. Geological Survey.

Purpose and Scope

The purpose of this report is to describe the specific sensor or sensing system, test its performance in three categories, complete related data analyses to quantify these performances, and report the results in a standardized document. In this chapter, the Pléiades Neo sensor is described. The performance of the system is limited to geometric, radiometric, and spatial. The scope of the geometric assessment is limited to testing the interior alignments of spectral bands against each other, and the exterior alignment is tested in reference to Sentinel-2 and to ground control points (GCPs).

The U.S. Geological Survey (USGS) Earth Resources Observation and Science Cal/Val Center of Excellence (ECCOE) project, and the associated system characterization process used for this assessment, follows the USGS Fundamental Science Practices, which include maintaining data, information, and documentation needed to reproduce and validate the scientific analysis documented in this report. Additional information and guidance about Fundamental Science Practices and related resource information of interest to the public are available at <https://www.usgs.gov/office-of-science-quality-and-integrity/fundamental-science-practices>. For additional information related to this report, please contact ECCOE at eccoe@usgs.gov.

System Description

This section describes the satellite and operational details and provides information about the Pléiades Neo sensor.

Satellite and Operational Details

Pléiades Neo is a constellation of four identical very-high-resolution optical satellites operated by Airbus Defence and Space. The first two satellites, Pléiades Neo-3 and -4, were launched in April and August 2021, respectively. The next two satellites, launched in December 2022, did not reach orbit because of Vega-C launch vehicle failure. Pléiades Neo provides several technical improvements to previous Pléiades-HR satellites, including the addition of coastal aerosol (deep blue) and red edge spectral bands, with improved ground sample distance and swath. The Pléiades Neo satellites were designed and built by Airbus Defence and Space with the high-resolution, multispectral imager for Earth imaging and use the S950 optical satellite bus. The high-resolution sensor on Pléiades Neo collects Earth data in the visible and near-infrared region with six bands and a panchromatic band. The satellites can operate off nadir to achieve a revisit of less than 1 day. The satellite and operational details for Pléiades Neo are listed in [table 1](#).

Sensor Information

The imaging sensor details for Pléiades Neo are listed in [table 2](#). The relative spectral responses for the Pléiades Neo sensor are shown in [figure 1](#).

Table 1. Satellite and operational details for Pléiades Neo.

[kg, kilogram; Ahr, ampere hour; km, kilometer; °, degree; min, minute; <, less than; ±, plus or minus; m, meter; VNIR, visible and near infrared]

Product information	Pléiades Neo data
Satellite and operational information	
Product name	Top of Atmosphere reflectance
Satellite name	Pléiades Neo
Sensor name(s)	Pléiades Neo Imager
Lift-off mass	920 kg
Sensor type	Multispectral, visible, and infrared
Platform owner	Airbus Defence and Space
Power	Dual-wing gallium arsenide panels, 150 Ahr battery
Mission type	Global land-monitoring tasking mission
Launch date	April 29, 2021 (Pléiades Neo-3), August 17, 2021 (Pléiades Neo-4)
Expected lifetime	10 years
Operator	Airbus Defence and Space
Operational details	
Operating orbit	Sun synchronous
Orbital altitude range	620 km
Sensor angle altitude	97.9° inclination
Altitude and orbit control	3-axis stabilized
Orbit period	97.2 min
Imaging time	10:30 descending node
Temporal resolution	<1 day
Temporal coverage	2021 to 2023
Imaging angles	Side looking = ±52°
Ground sample distance(s)	0.30 m panchromatic; 1.2 m VNIR
Data licensing	Restricted
Data pricing	Commercial data pricing
Product abstract	https://www.intelligence-airbusds.com/imagery/constellation/pleiades-neo/how-to-order/user-guide
Product locator	https://www.intelligence-airbusds.com/contact/oneatlas

Table 2. Imaging sensor details for Pléiades Neo.

[µm, micrometer; m, meter; NIR, near infrared]

Spectral band details	Pléiades Neo			
	Lower band (µm)	Upper band (µm)	Radiometric resolution (bits)	Ground sample distance (m)
Band 1—Panchromatic	0.450	0.800	12	0.3
Band 2—Coastal aerosol	0.400	0.460	12	1.2
Band 3—Blue	0.460	0.520	12	1.2
Band 4—Green	0.520	0.600	12	1.2
Band 5—Red	0.600	0.680	12	1.2
Band 6—Red edge	0.680	0.720	12	1.2
Band 7—NIR	0.730	0.900	12	1.2

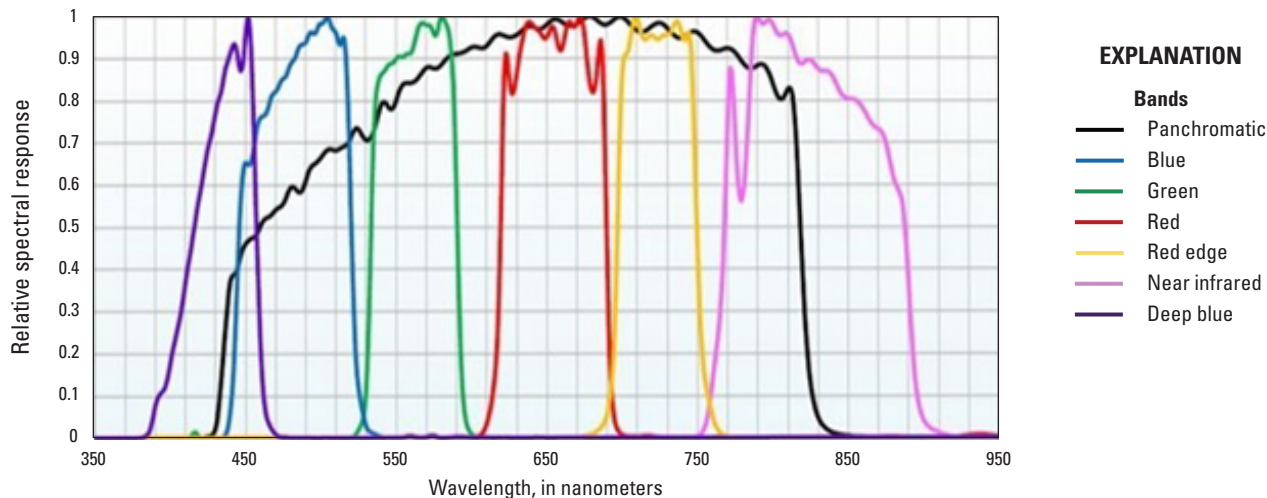


Figure 1. Pléiades Neo visible and near-infrared relative spectral response (image courtesy of Airbus Defence and Space; used with permission).

Procedures

ECCOE has established standard processes to identify Earth observing systems of interest and to assess the geometric, radiometric, and spatial qualities of data products from these systems.

The assessment steps are as follows:

- system identification and investigation to learn the general specifications of the satellite and its sensor(s);
- data receipt and initial inspection to understand the characteristics and any overt flaws in the data product so that it may be further analyzed;
- geometric characterization, including interior geometric orientation measuring the relative alignment of spectral bands and exterior geometric orientation measuring how well the georeferenced pixels within the image are aligned to a known reference;

- radiometric characterization, including assessing how well the data product correlates with a known reference and, when possible, assessing the signal-to-noise ratio; and
- spatial characterization, assessing the two-dimensional fidelity of the image pixels to their projected GSD.

Data analysis and test results are maintained at the USGS Earth Resources Observation and Science Center by the ECCOE project.

Measurements

The observed USGS measurements are listed in [table 3](#). Physical error, in meters, is calculated by the GSD (1.2-m VNIR band to band, 10.0-m VNIR image to image) multiplied by the pixel error. Details about the methodologies used are outlined in the “Analysis” section.

Table 3. U.S. Geological Survey measurement results.

[RMSE, root mean square error; m, meter; NIR, near infrared; FWHM, full width at half maximum; MTF, modulation transfer function; USGS, U.S. Geological Survey; NED, near infrared, red edge, and deep blue (coastal aerosol); ~, about; %, percent]

Description of product	Top of Atmosphere reflectance
Geometric performance (mean error, RMSE), in meters (pixels) in easting, northing	
Interior (band to band)	Band 3 (blue)
	Mean: 0.007 m (0.006), 0.010 m (0.008)
	RMSE: 0.021 m (0.018), 0.023 m, (0.019)
	Band 4 (green)
	Mean: 0.001 m (0.0008), 0.003 m (0.0025)
	RMSE: 0.019 m (0.016), 0.021 m, (0.018)
	Band 7 (NIR)
	Mean: -0.006 m (-0.005), -0.017 m (-0.014)
	RMSE: 0.024 m (0.020), 0.032 m, (0.027)
Exterior (geometric location accuracy)	NIR—Mean: -1.49 m (-0.149), 2.21 m (0.221)
	NIR—RMSE: 6.38 m (0.636), 3.13 m (0.313)
Radiometric performance (offset, slope)	
Radiometric evaluation (linear regression— Pléiades Neo versus Sentinel-2 reflectance)	Band 3—Blue (offset, slope): -0.053, 1.107
	Band 4—Green (offset, slope): -0.070, 1.202
	Band 5—Red (offset, slope): -0.066, 1.140
	Band 7—NIR (offset, slope): -0.063, 1.155
Spatial performance	
Spatial performance measurement	Band 2—Coastal aerosol: FWHM = 1.002 pixels; MTF at Nyquist = 0.3422
	Band 3—Blue: FWHM = 1.054 pixels; MTF at Nyquist = 0.3110
	Band 4—Green: FWHM = 1.226 pixels; MTF at Nyquist = 0.2231
	Band 5—Red: FWHM = 1.087 pixels; MTF at Nyquist = 0.2924
	Band 7—NIR: FWHM = 1.149 pixels; MTF at Nyquist = 0.2597
Known artifacts and quality issues	
USGS noted artifacts/quality issues ¹	Band 2—Coastal aerosol gain is considerably lower than other NED gains
	Bands 6 and 7—Red edge and NIR (~50% lower)

¹These were known issues at the time of analysis in October 2022. We acknowledge these issues may have since been resolved.

Analysis

This section of the report describes the geometric, radiometric, and spatial performance of Pléiades Neo.

Geometric Performance

The geometric performance results for Pléiades Neo are characterized in terms of the interior (band-to-band alignment) and exterior (geometric location accuracy) geometric analysis results.

Interior (Band to Band)

The interior, or band-to-band alignment, analysis was completed on four images over the United States and China: (1) an image taken over Boulder, Colorado (scene identifier PNEO4_202208101755205_MS-FS_SEN); (2) an image taken over Baotou, Inner Mongolia, China (scene identifier PNEO3_202203310331286_MS-FS_SEN); (3) an image taken over Sioux Falls, South Dakota (scene identifier PNEO4_202203261720599_PMS-FS_SEN); and (4) an image taken over Fort Lupton, Colo. (scene identifier

PNEO3_202110201751341_MS-FS_SEN). Band combinations were registered against each other to determine the mean error, root mean square error, and standard deviation, as listed in table 4, with results represented in pixels at a 1.2-m VNIR and a 0.3-m panchromatic GSD. Geometric error maps for each assessed VNIR band combination for the Boulder image, as well as the corresponding histogram graphs and plots, are shown in figures 2 through 10. The geometric error maps indicate the directional shift and relative magnitude of the shift, whereas the histogram graphs indicate frequency of observed mean error measurements within the image. Geometric error maps for each assessed VNIR band combination for the Baotou image, as well as the corresponding histogram graphs, are shown in figures 11 through 19. Geometric error maps for each assessed VNIR band combination for the Sioux Falls image, as well as the corresponding histogram graphs, are shown in figures 20 through 28. Geometric error maps for each assessed VNIR band combination for the Fort Lupton image, as well as the corresponding histogram graphs and plots, are shown in figures 29 through 37. Together, the interior and exterior geometric analysis results, as reported in the “Interior (Band to Band)” and “Exterior (Geometric Location Accuracy)” sections, provide a comprehensive assessment of geometric accuracy.

Table 4. Band-to-band registration error (in pixels).

[STD, standard deviation; RMSE, root mean square error; NIR, near infrared]

Image	Band combination	Mean error (easting)	Mean error (northing)	STD (easting)	STD (northing)	RMSE (easting)	RMSE (northing)
Boulder, Colorado	Blue–green	0.005	0.007	0.025	0.023	0.026	0.024
	Green–red	–0.002	0.007	0.026	0.025	0.026	0.026
	Red edge–NIR	–0.023	–0.043	0.033	0.041	0.041	0.059
Baotou, Inner Mongolia, China	Blue–green	0.004	0.008	0.010	0.013	0.011	0.015
	Green–red	–0.001	–0.000	0.008	0.010	0.008	0.010
	Red edge–NIR	–0.001	–0.007	0.009	0.012	0.009	0.014
Sioux Falls, South Dakota	Blue–green	0.015	0.022	0.018	0.021	0.024	0.030
	Green–red	0.002	0.009	0.019	0.021	0.019	0.023
	Red edge–NIR	–0.005	–0.006	0.021	0.027	0.021	0.028
Fort Lupton, Colorado	Blue–green	0.005	0.003	0.020	0.021	0.021	0.021
	Green–red	0.005	–0.005	0.022	0.024	0.023	0.025
	Red edge–NIR	0.004	–0.011	0.023	0.023	0.024	0.026

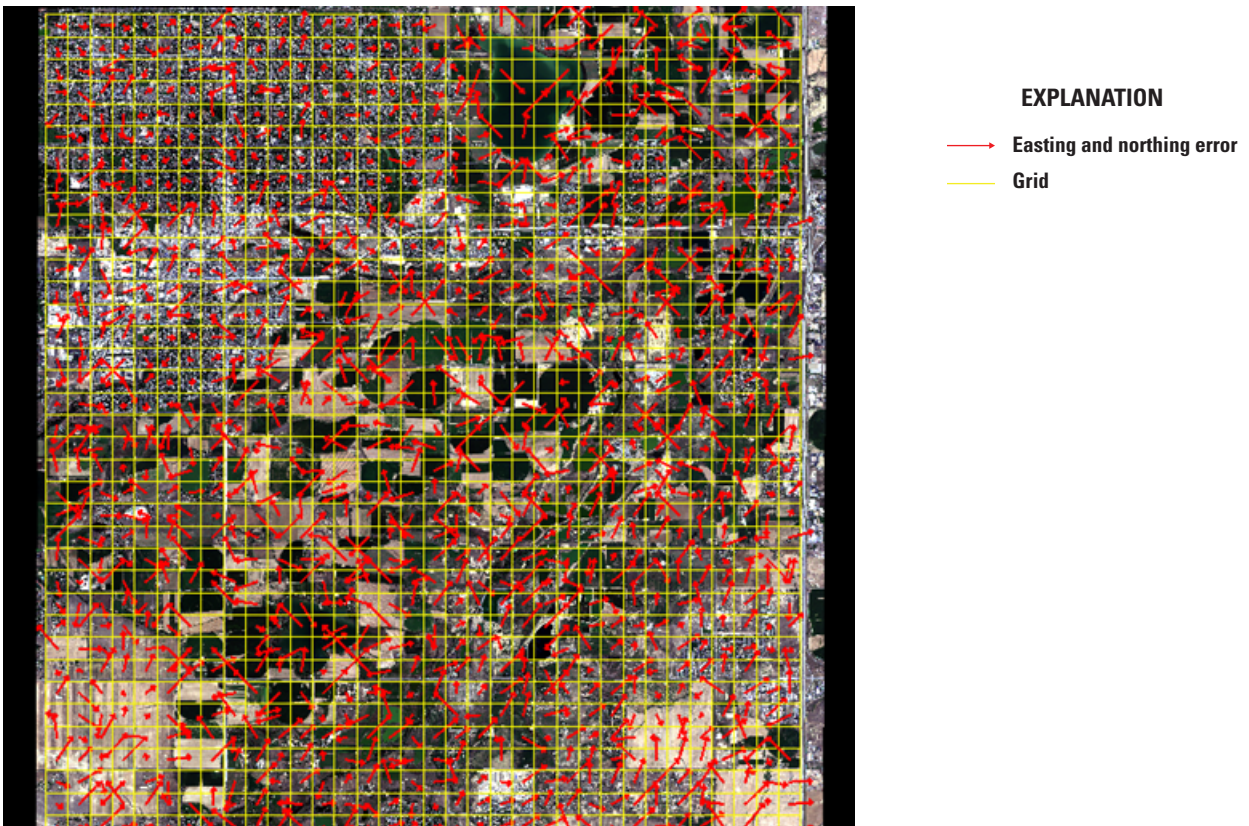


Figure 2. Band 3 (blue) to band 4 (green) geometric error map of Boulder, Colorado.

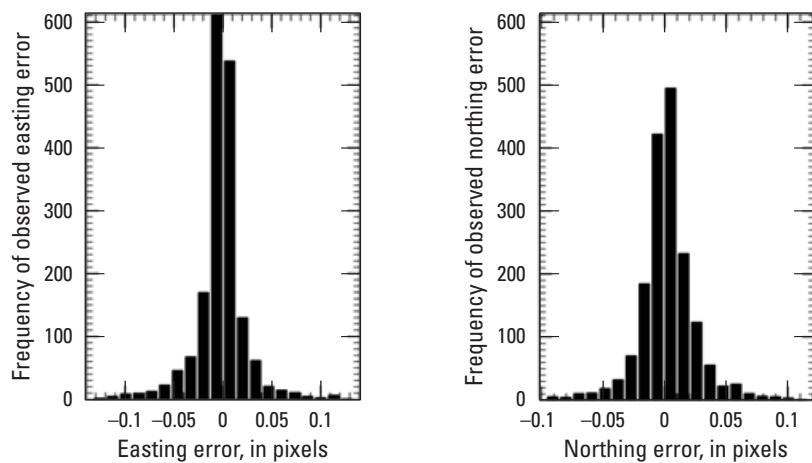


Figure 3. Band 3 (blue) to band 4 (green) geometric error histogram for Boulder, Colorado.

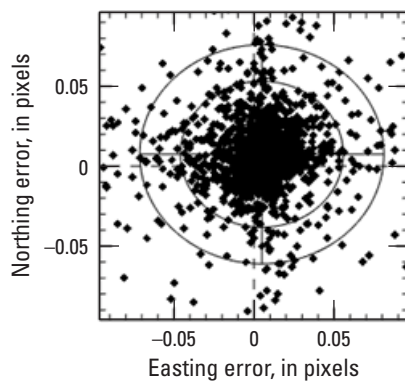


Figure 4. Band 3 (blue) to band 4 (green) geometric error plot for Boulder, Colorado.

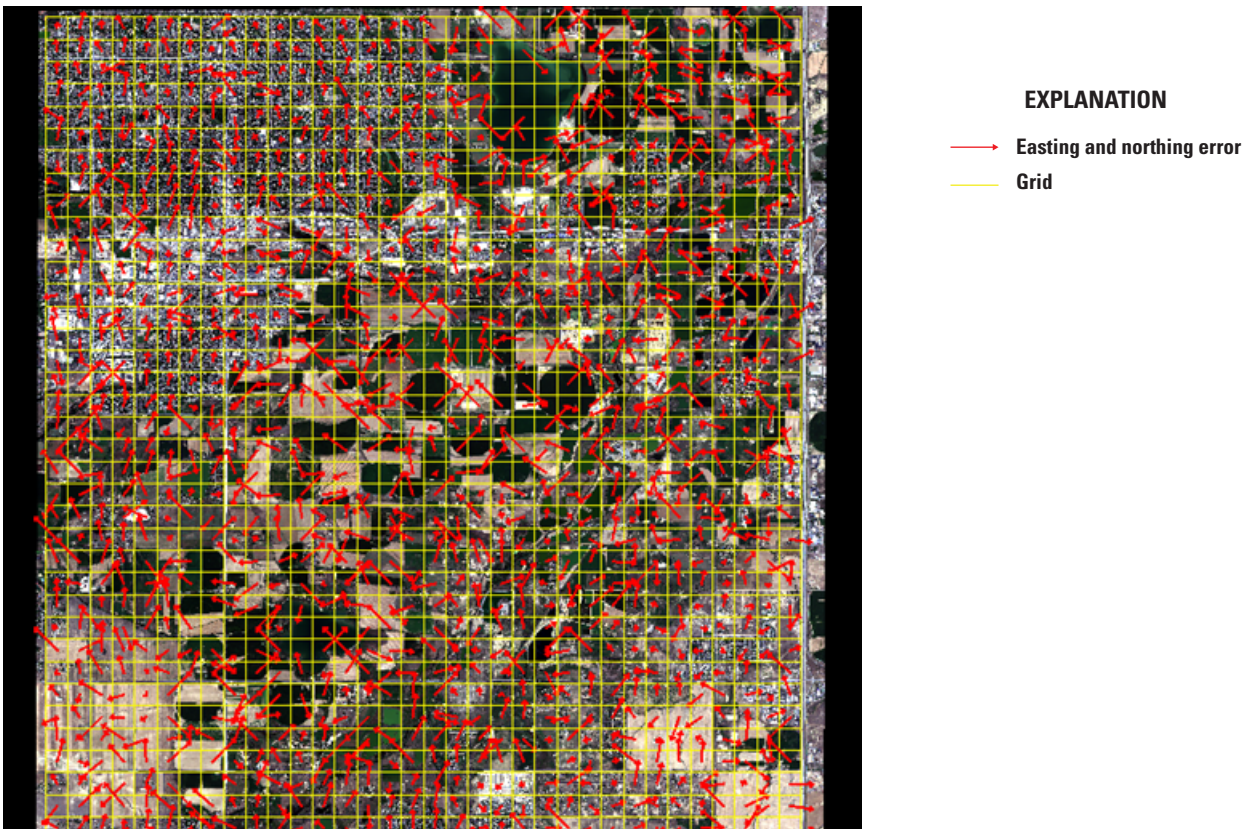


Figure 5. Band 4 (green) to band 5 (red) geometric error map of Boulder, Colorado.

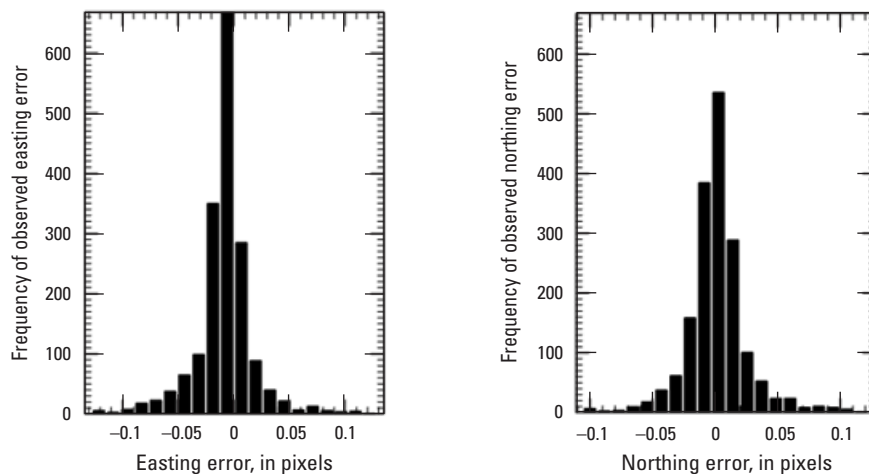


Figure 6. Band 4 (green) to band 5 (red) geometric error histogram for Boulder, Colorado.

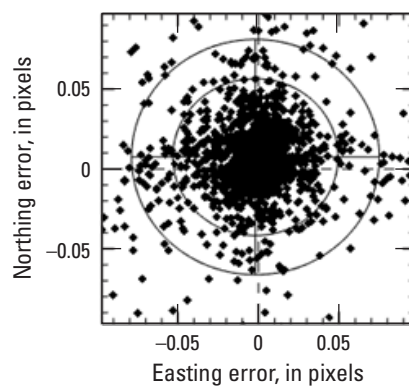


Figure 7. Band 4 (green) to band 5 (red) geometric error plot for Boulder, Colorado.

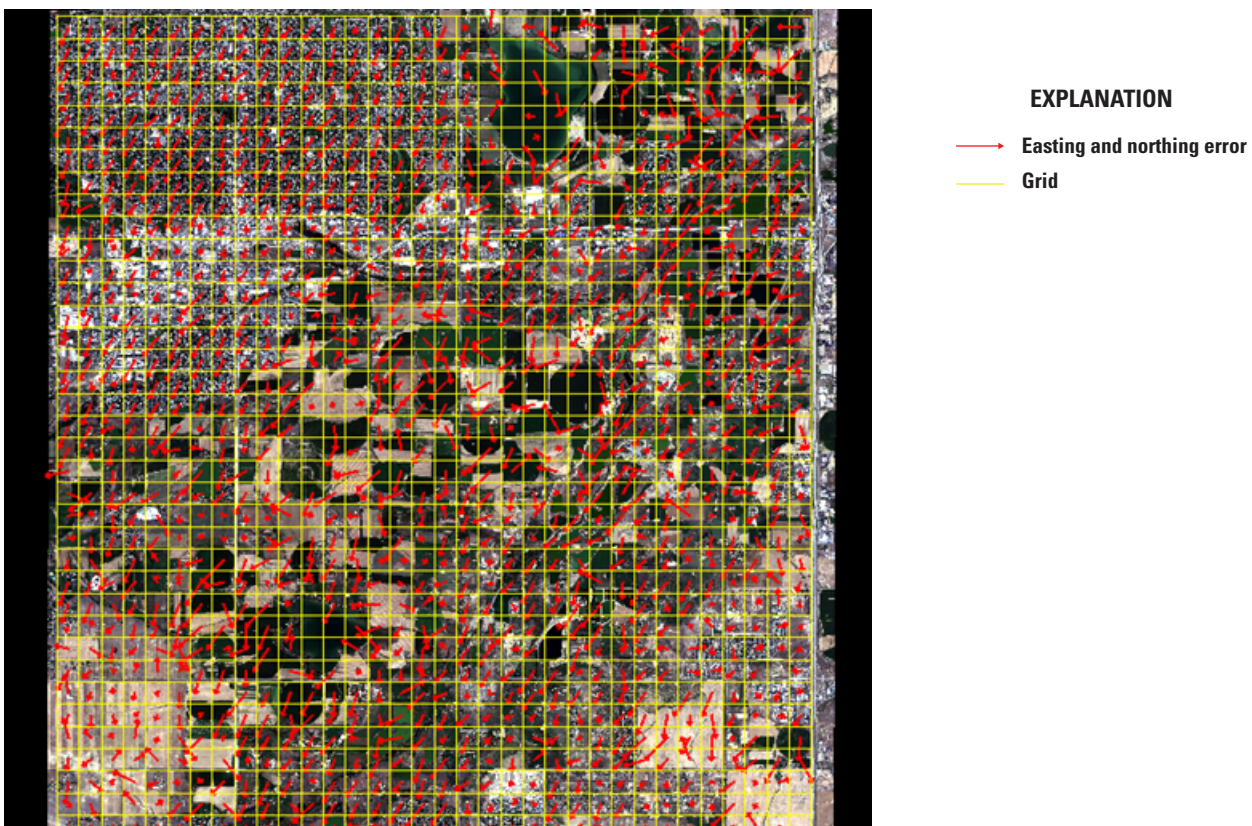


Figure 8. Band 6 (red edge) to band 7 (near infrared) geometric error map of Boulder, Colorado.

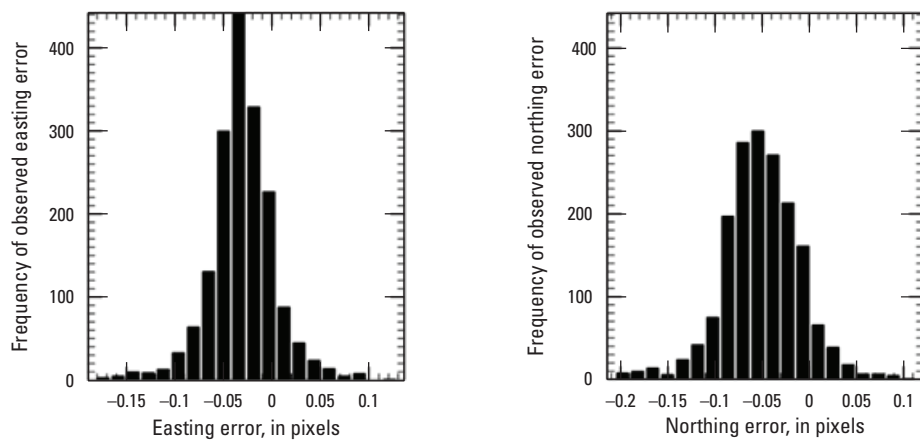


Figure 9. Band 6 (red edge) to band 7 (near infrared) geometric error histogram for Boulder, Colorado.

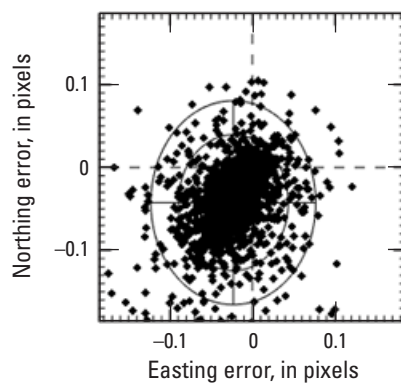


Figure 10. Band 6 (red edge) to band 7 (near infrared) geometric error plot for Boulder, Colorado.

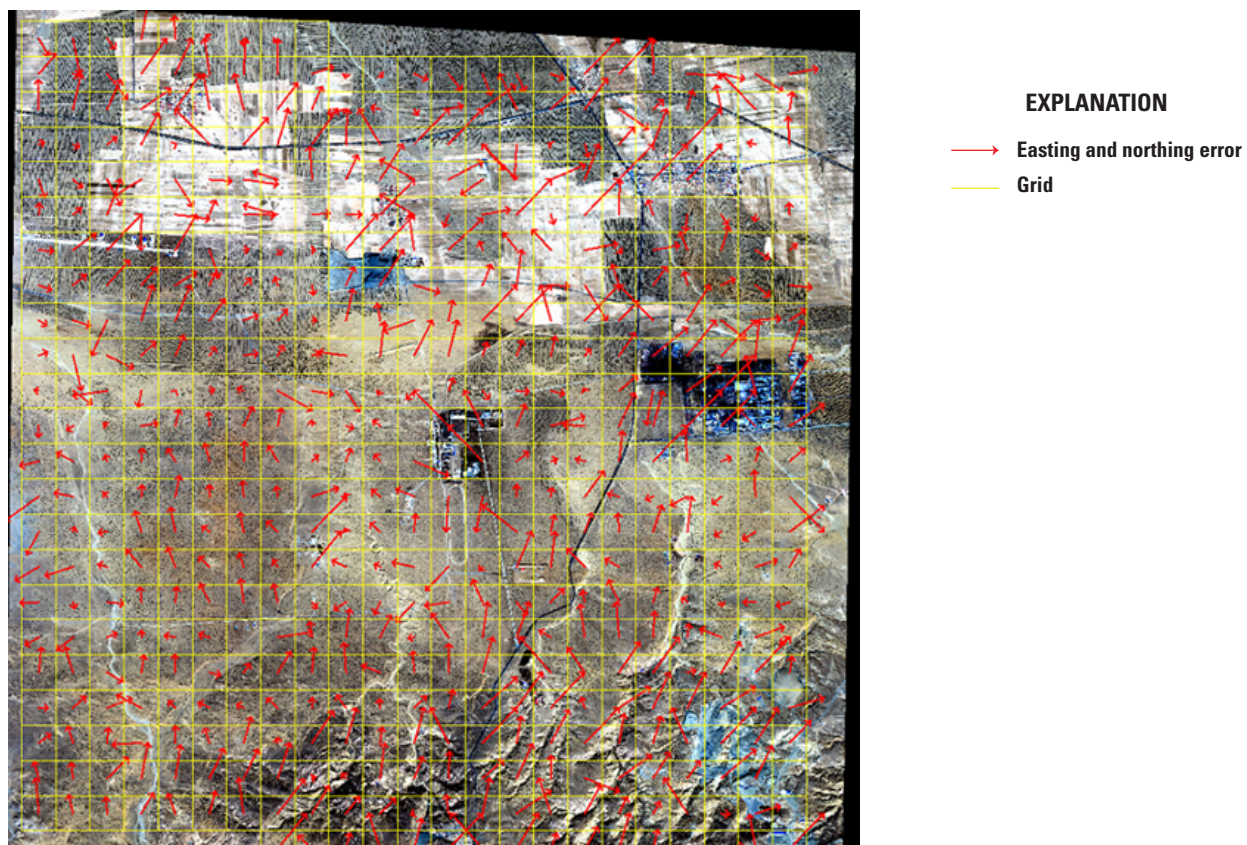


Figure 11. Band 3 (blue) to band 4 (green) geometric error map of Baotou, Inner Mongolia, China.

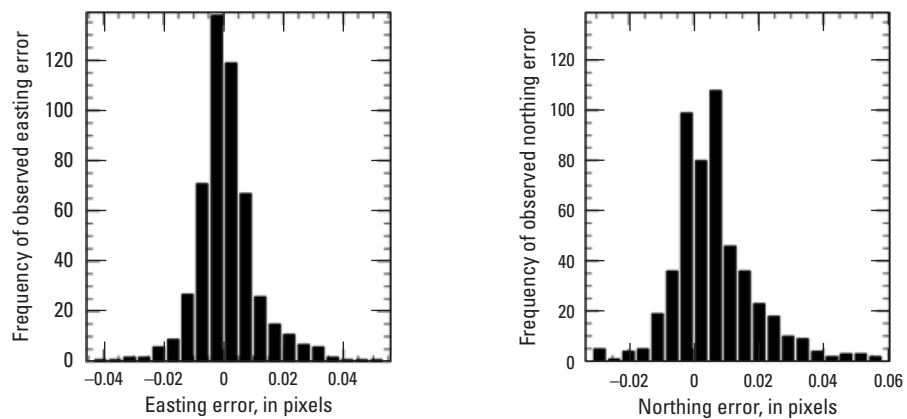


Figure 12. Band 3 (blue) to band 4 (green) geometric error histogram for Baotou, Inner Mongolia, China.

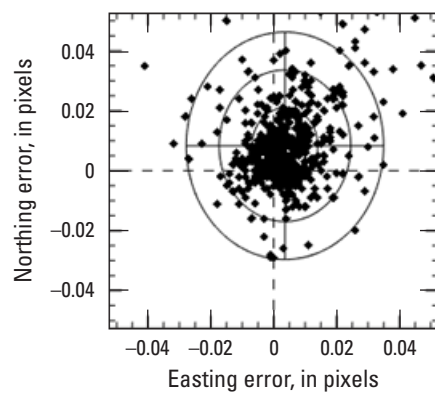


Figure 13. Band 3 (blue) to band 4 (green) geometric error plot for Baotou, Inner Mongolia, China.

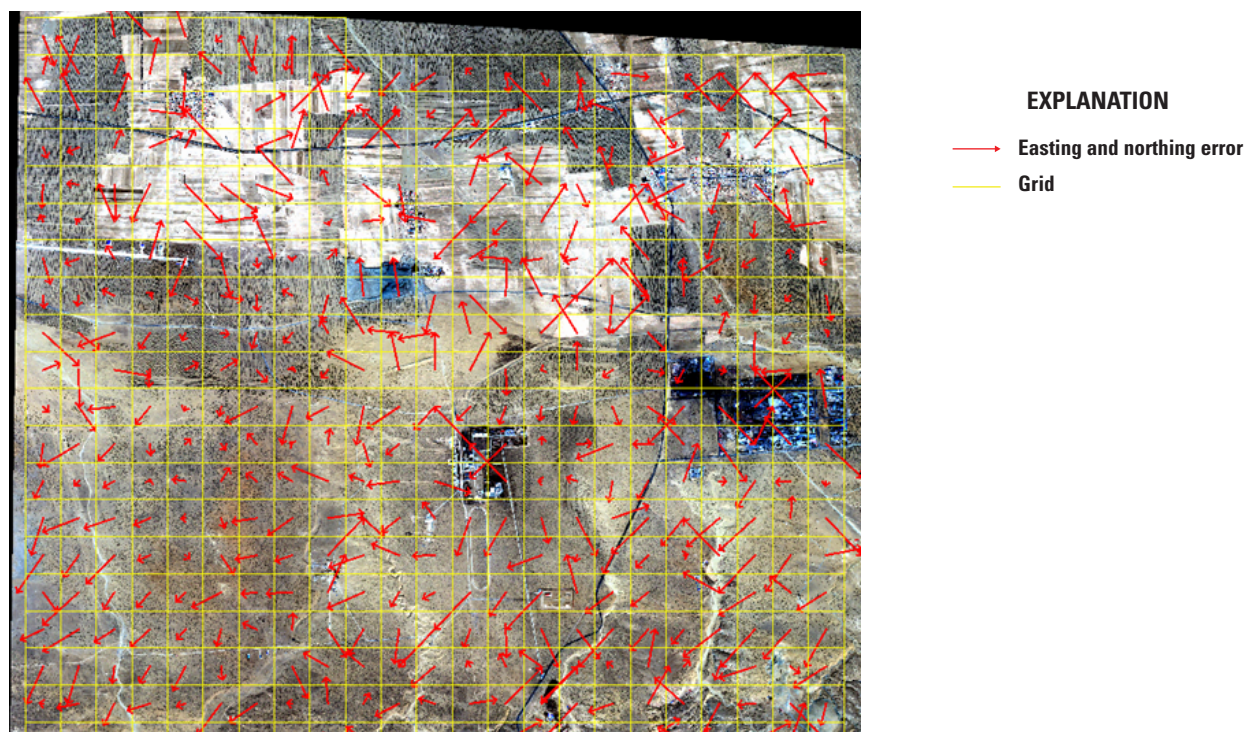


Figure 14. Band 4 (green) to band 5 (red) geometric error map for Baotou, Inner Mongolia, China.

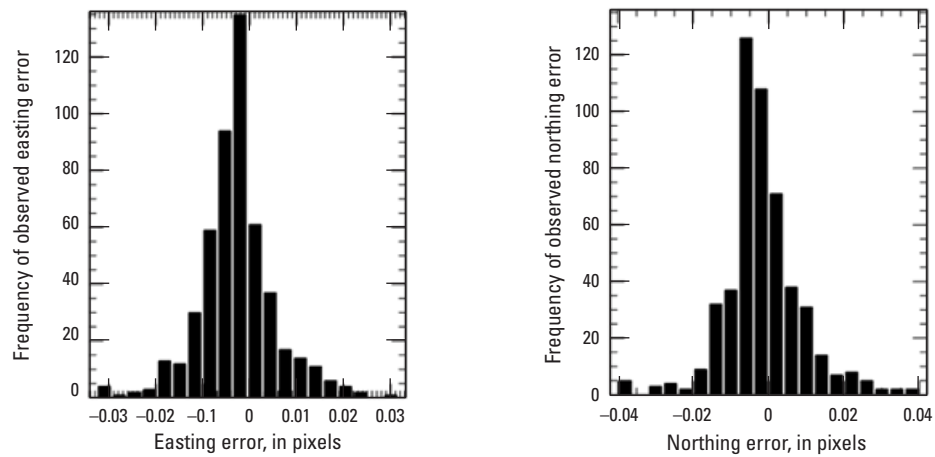


Figure 15. Band 4 (green) to band 5 (red) geometric error histogram for Baotou, Inner Mongolia, China.

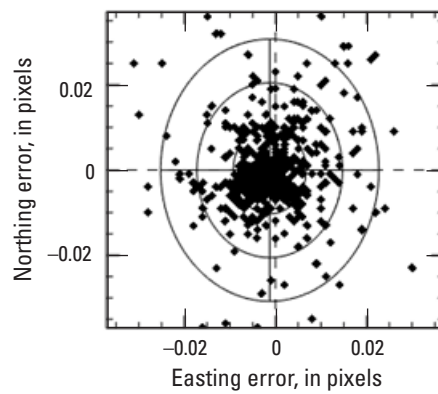


Figure 16. Band 4 (green) to band 5 (red) geometric error plot for Baotou, Inner Mongolia, China.

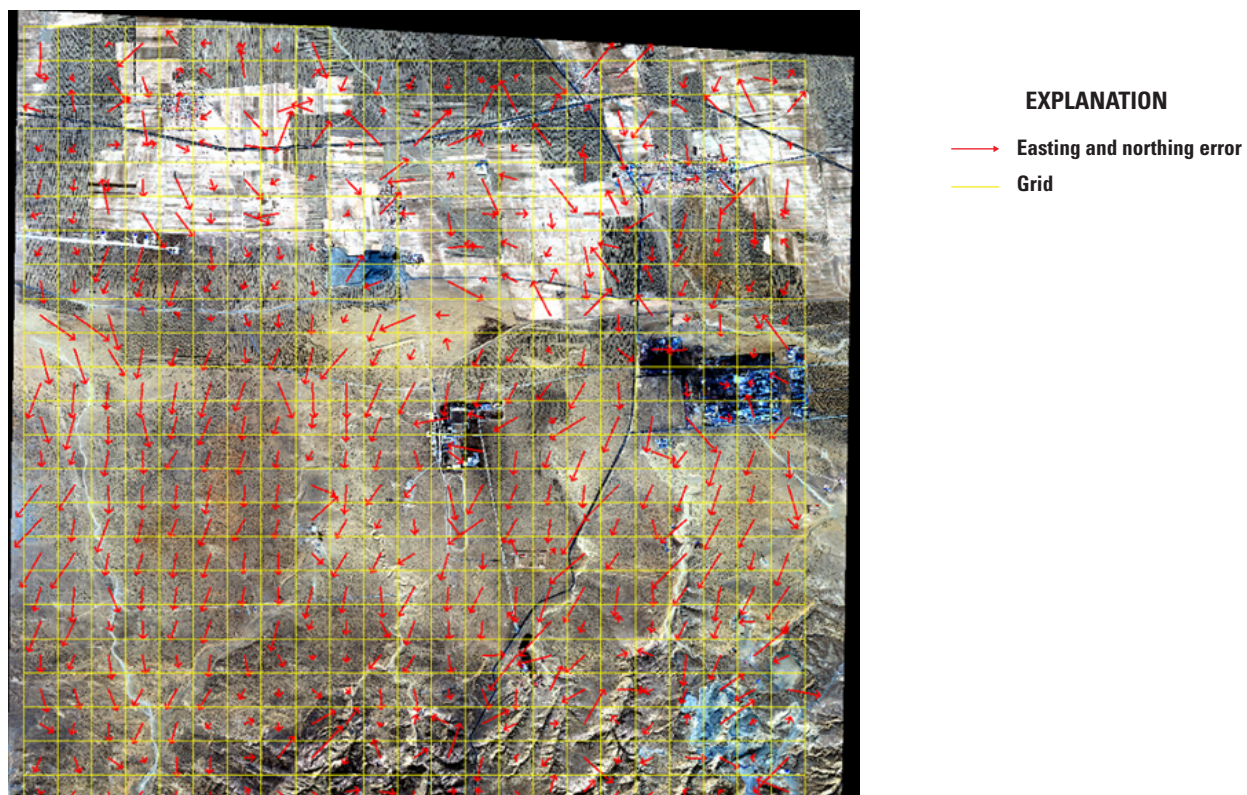


Figure 17. Band 6 (red edge) to band 7 (near infrared) geometric error map of Baotou, Inner Mongolia, China.

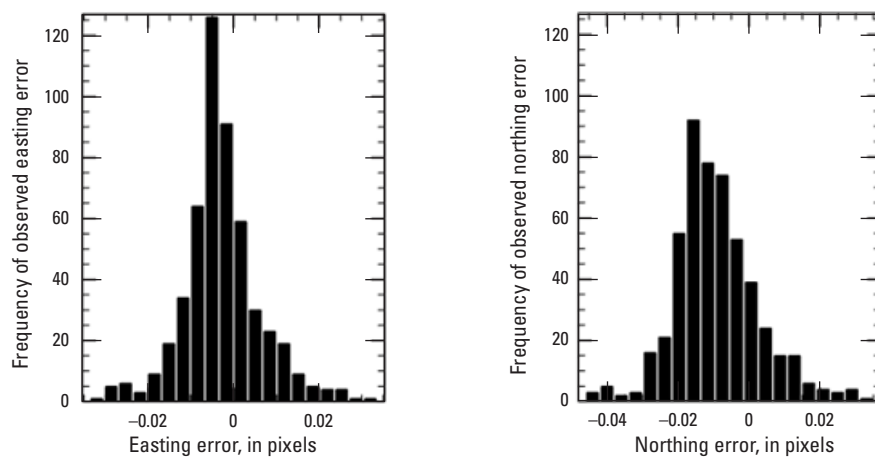


Figure 18. Band 6 (red edge) to band 7 (near infrared) geometric error histogram for Baotou, Inner Mongolia, China.

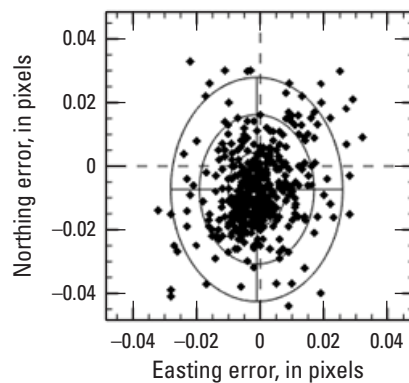


Figure 19. Band 6 (red edge) to band 7 (near infrared) geometric error plot for Baotou, Inner Mongolia, China.

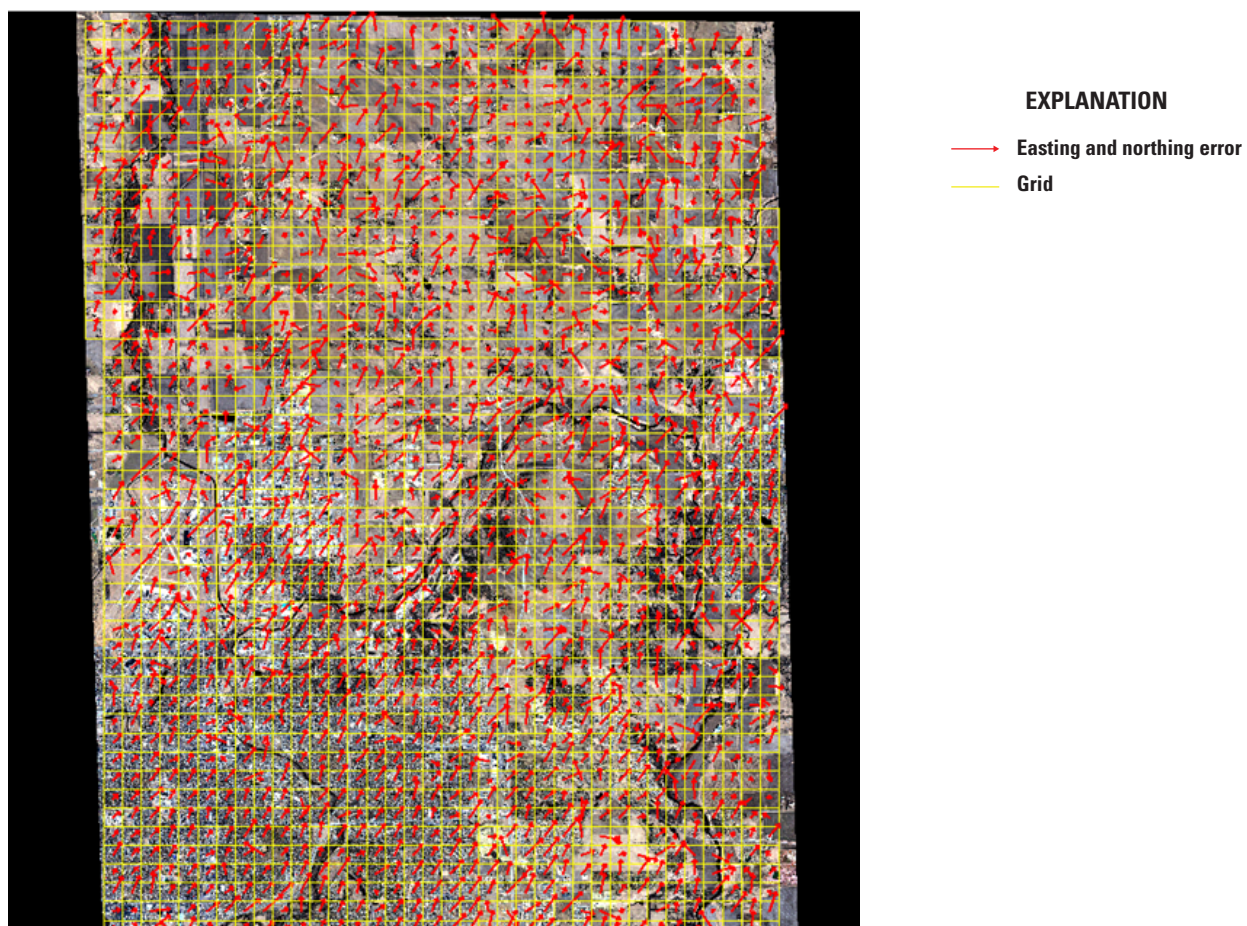


Figure 20. Band 3 (blue) to band 4 (green) geometric error map for Sioux Falls, South Dakota.

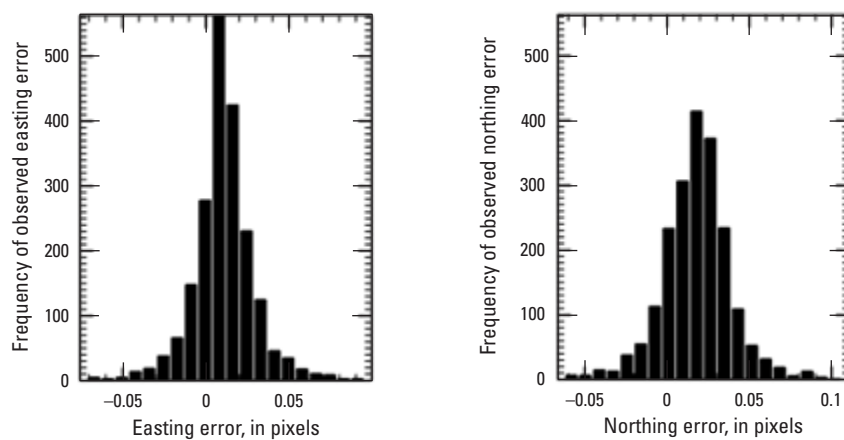


Figure 21. Band 3 (blue) to band 4 (green) geometric error histogram of Sioux Falls, South Dakota.

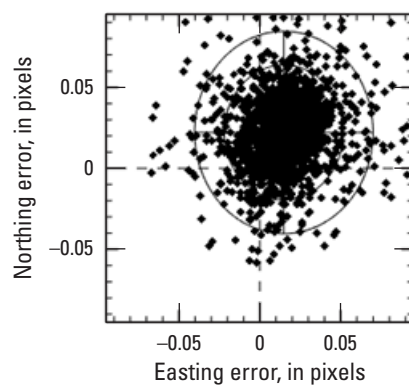


Figure 22. Band 3 (blue) to band 4 (green) geometric error plot for Sioux Falls, South Dakota.

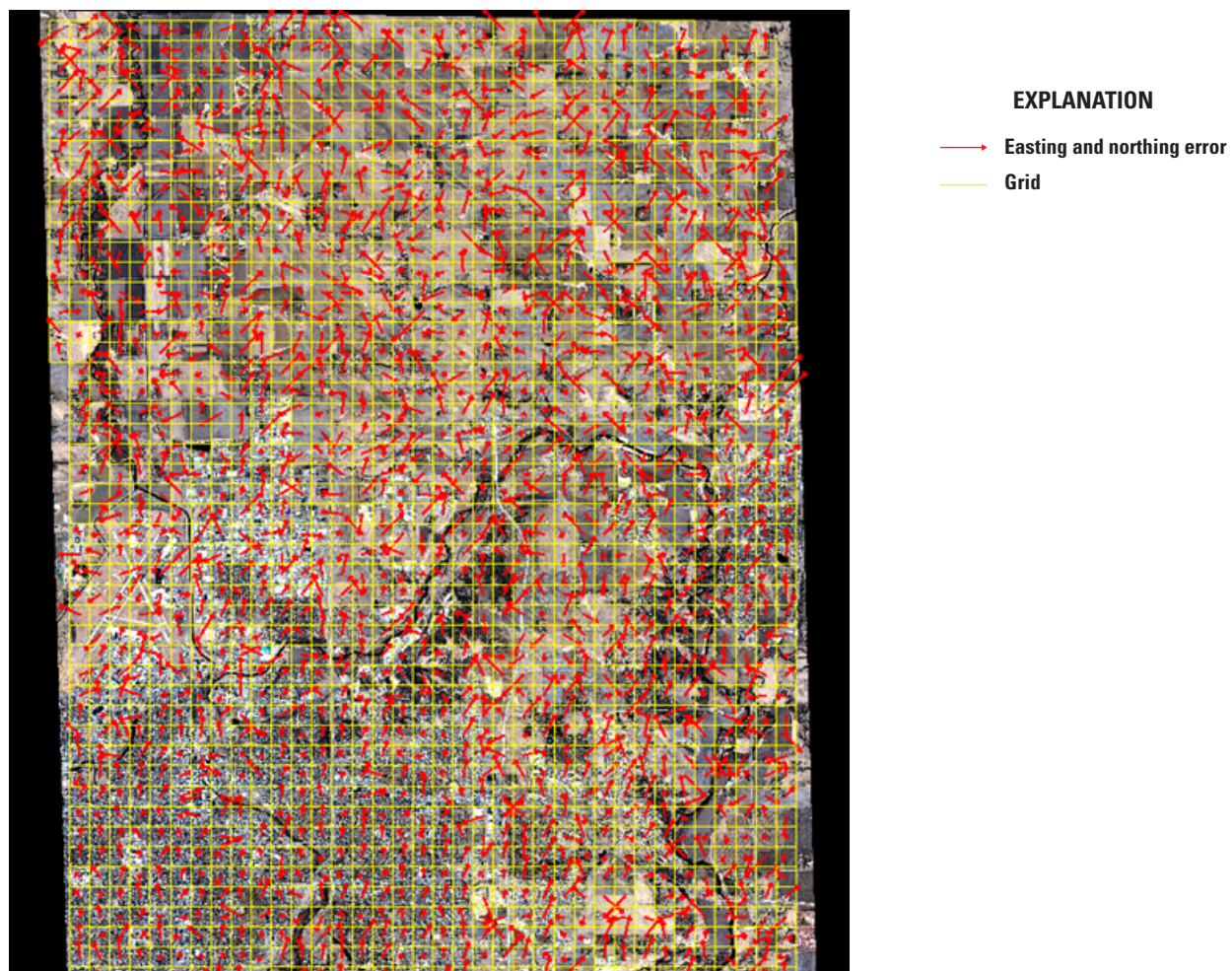


Figure 23. Band 4 (green) to band 5 (red) geometric error map for Sioux Falls, South Dakota.

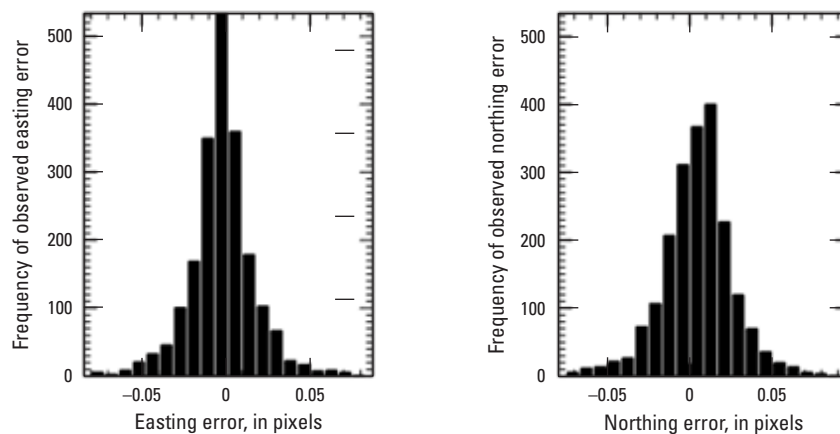


Figure 24. Band 4 (green) to band 5 (red) geometric error histogram for Sioux Falls, South Dakota.

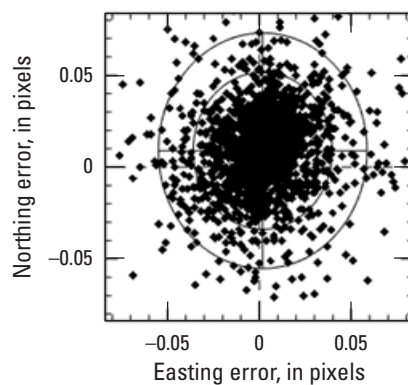


Figure 25. Band 4 (green) to band 5 (red) geometric error plot for Sioux Falls, South Dakota.

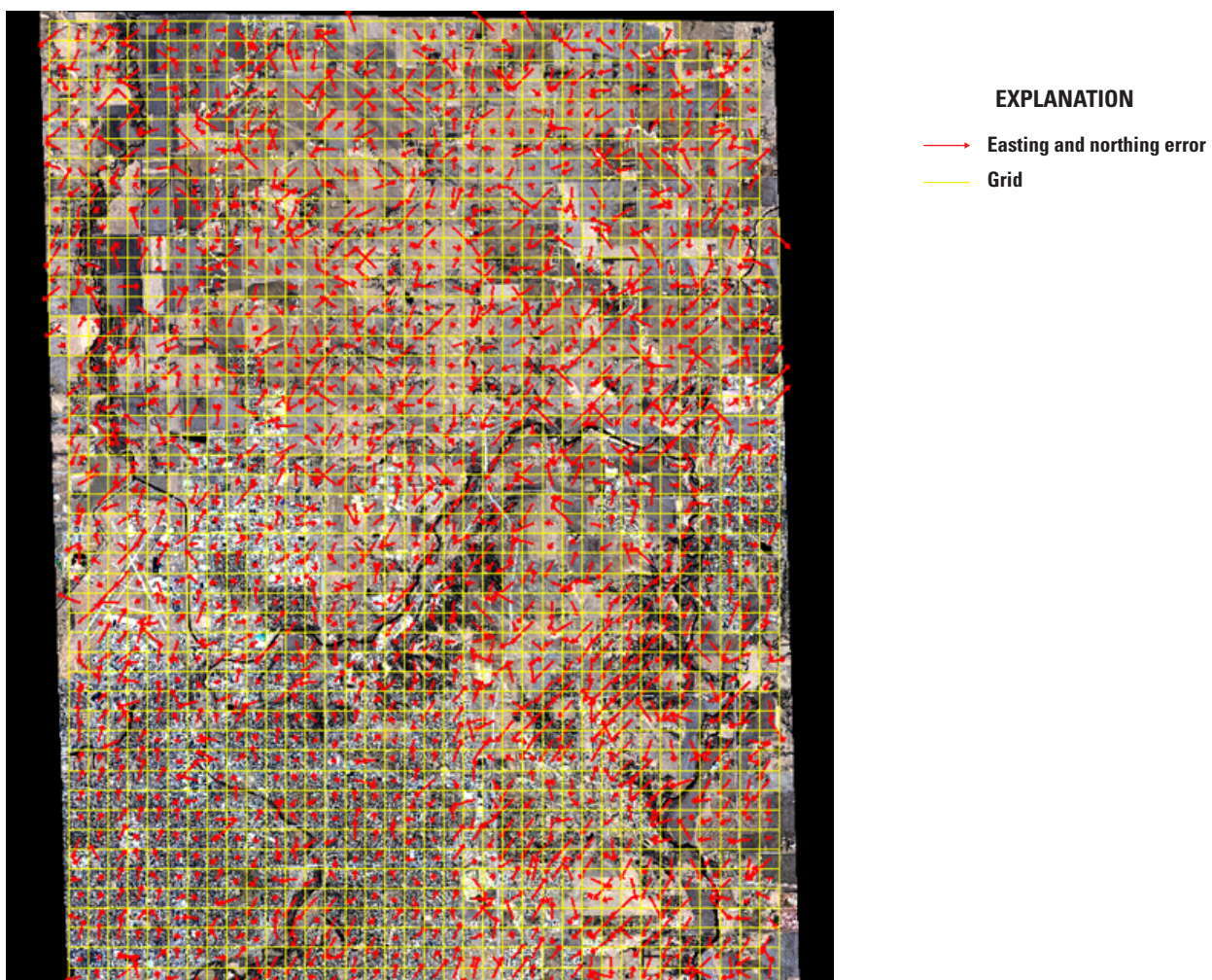


Figure 26. Band 6 (red edge) to band 7 (near infrared) geometric error map for Sioux Falls, South Dakota.

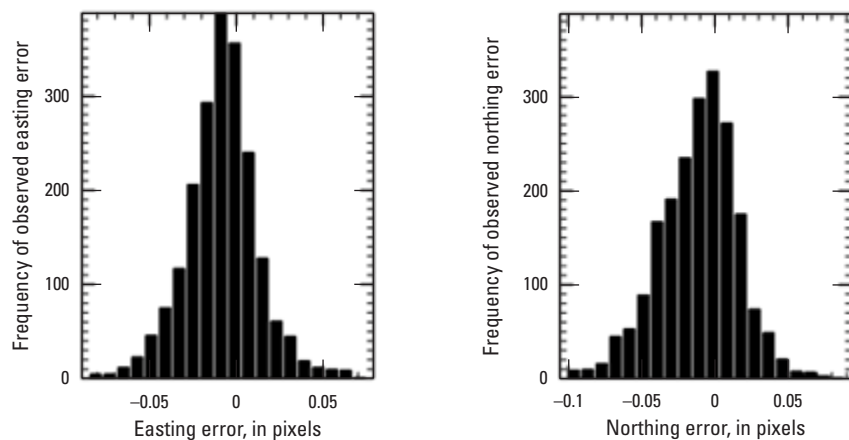


Figure 27. Band 6 (red edge) to band 7 (near infrared) geometric error histogram for Sioux Falls, South Dakota.

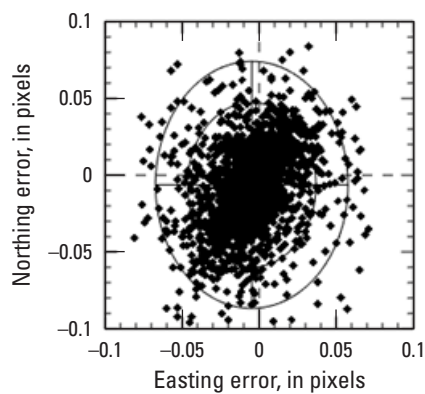


Figure 28. Band 6 (red edge) to band 7 (near infrared) geometric error plot for Sioux Falls, South Dakota.

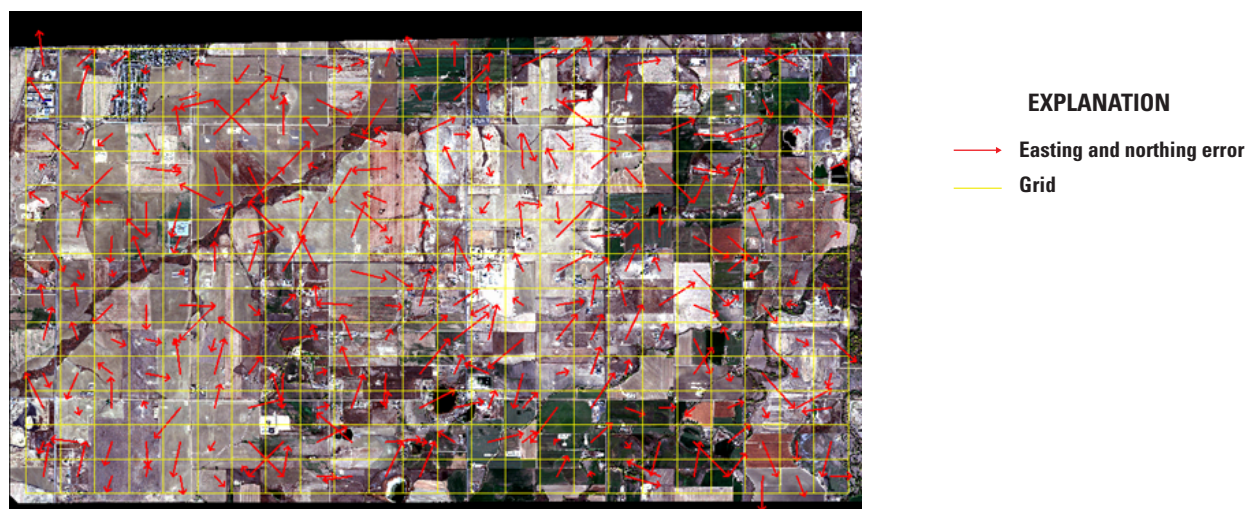


Figure 29. Band 3 (blue) to band 4 (green) geometric error map for Fort Lupton, Colorado.

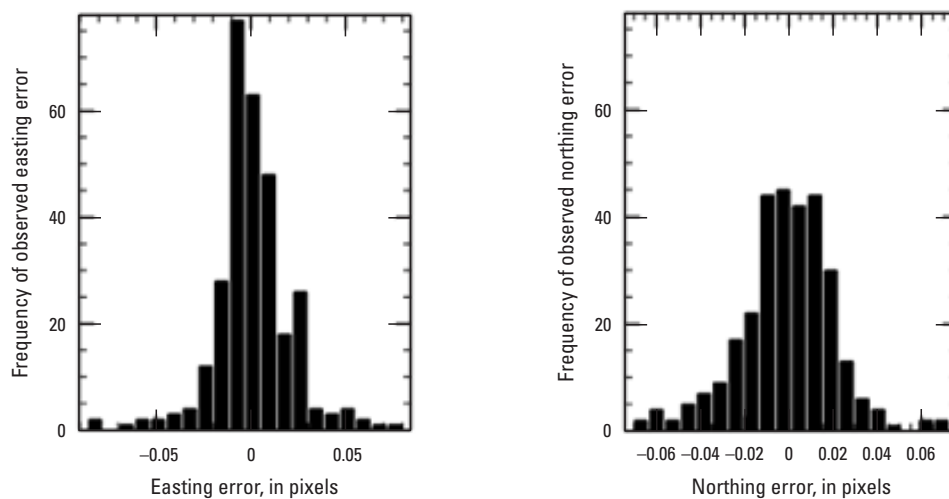


Figure 30. Band 3 (blue) to band 4 (green) geometric error histogram of Fort Lupton, Colorado.

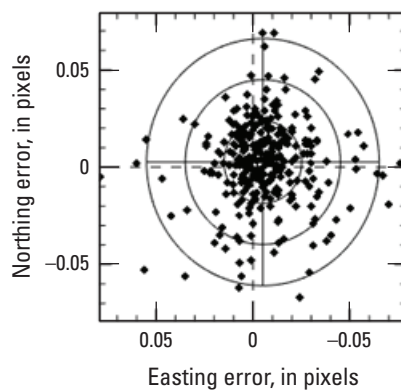


Figure 31. Band 3 (blue) to band 4 (green) geometric error plot for Fort Lupton, Colorado.

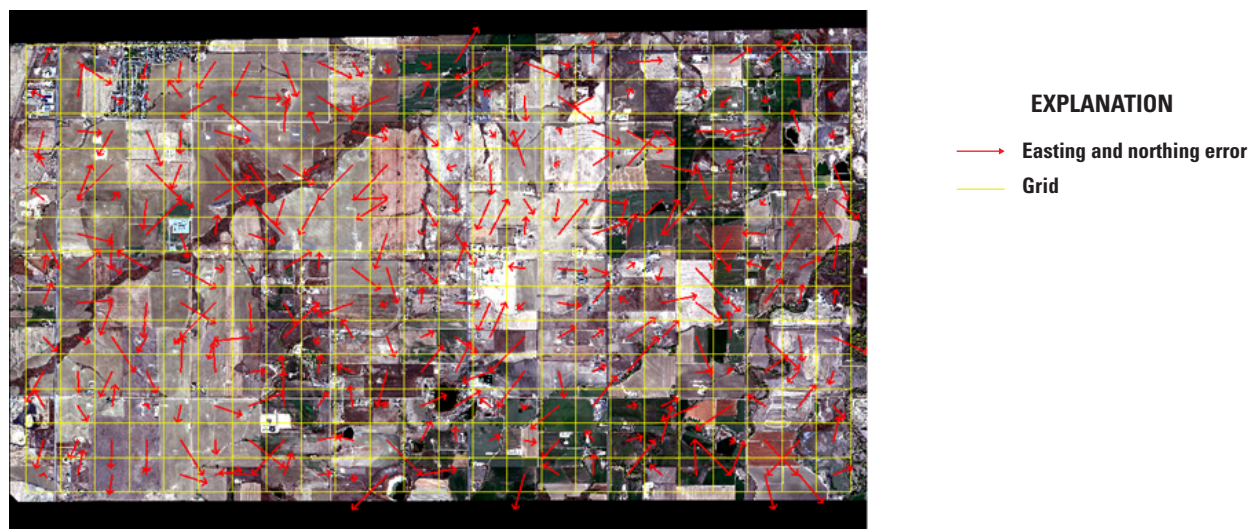


Figure 32. Band 4 (green) to band 5 (red) geometric error map for Fort Lupton, Colorado.

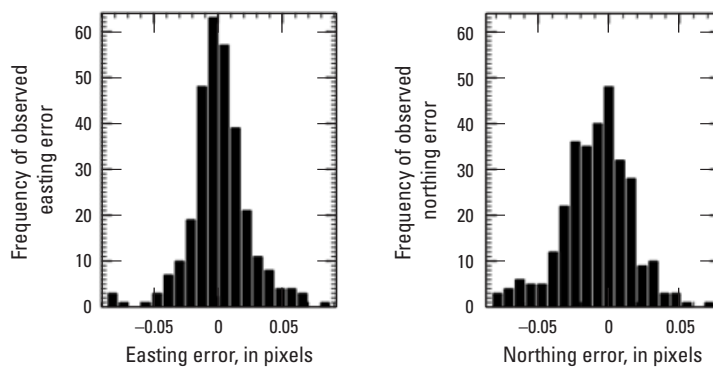


Figure 33. Band 4 (green) to band 5 (red) geometric error histogram for Fort Lupton, Colorado.

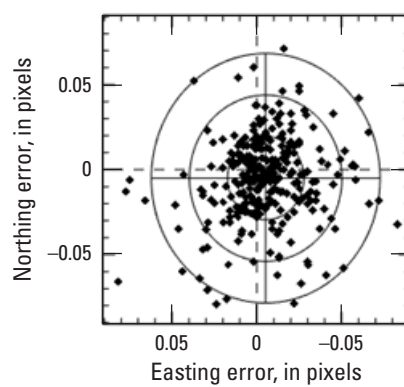


Figure 34. Band 4 (green) to band 5 (red) geometric error plot for Fort Lupton, Colorado.

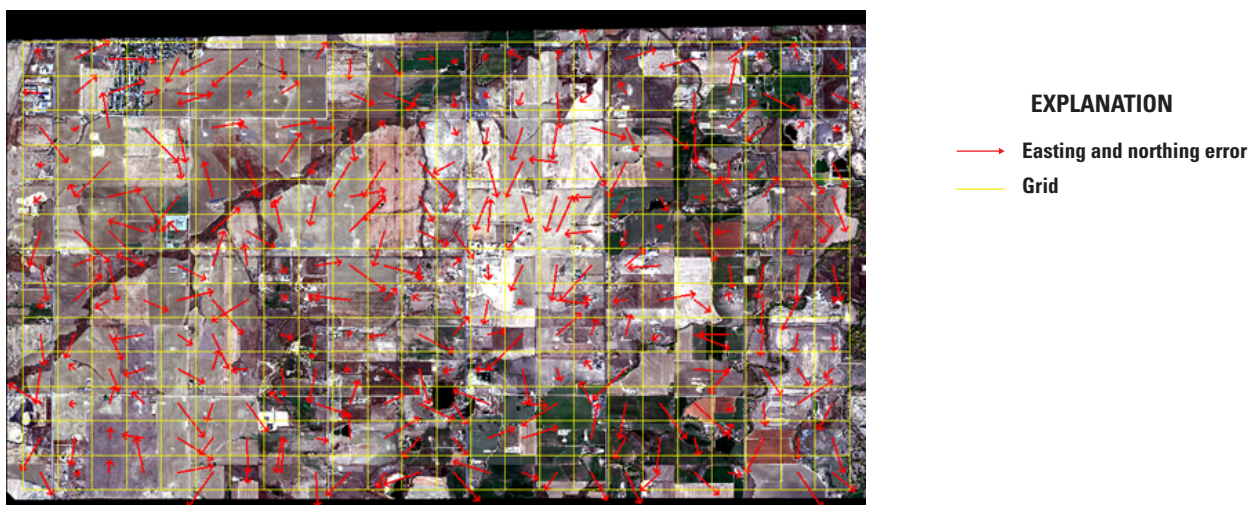


Figure 35. Band 6 (red edge) to band 7 (near infrared) geometric error map for Fort Lupton, Colorado.

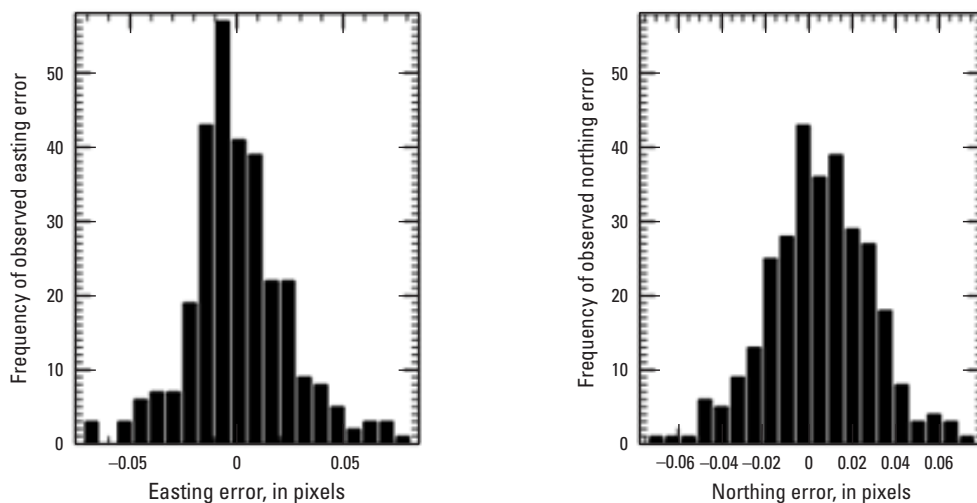


Figure 36. Band 6 (red edge) to band 7 (near infrared) geometric error histogram for Fort Lupton, Colorado.

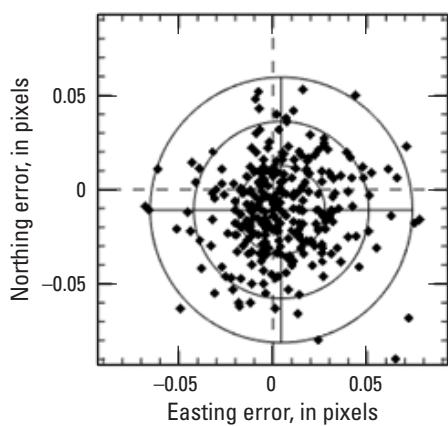


Figure 37. Band 6 (red edge) to band 7 (near infrared) geometric error plot for Fort Lupton, Colorado.

Exterior (Geometric Location Accuracy)

For this analysis, two procedures were used. In the first procedure, the exterior, or geometric location accuracy, analysis was completed on two Pléiades Neo images over the United States: (1) an image taken over Fort Lupton, Colo. (scene identifier PNEO3_202110201751341_MS-FS_SEN), and (2) a new Pléiades Neo image taken over Sioux Falls, S. Dak. (scene identifier PNEO4_202205121724235_MS-FS_SEN), that was selected for this analysis. Three orthorectified scenes over the United States and China were also selected for this analysis: (1) an image taken over Baotou, Inner Mongolia, China (scene identifier PNEO3_202203310331286_MS-FS_ORT); (2) an image taken over Sioux Falls, S. Dak. (scene identifier PNEO4_202205121724235_MS-FS_ORT); and (3) an image taken over Fort Lupton, Colo. (scene identifier PNEO3_202110201751340_MS-FS_ORT). For this analysis, band 7 (near infrared) of the Pléiades Neo data was compared against the corresponding band from three Sentinel-2 images: (1) an image taken over Baotou, Inner Mongolia, China (scene identifier L1C_T49TCF_A026499_20220403T033449); (2) an image taken over Sioux Falls, S. Dak. (scene identifier L1C_T14TPP_A027065_20220512T172742); and (3) an image taken over Fort Lupton, Colo. (scene identifier L1C_T13TEE_A024148_20211020T174348).

Conjugate points in the reference and search images were identified automatically and refined using similarity measures such as normalized cross-correlation metrics, and the mean error and standard deviation results are listed in [tables 5 and 6](#) with results represented in pixels at a 10-m GSD. For each of

the four images, geometric error maps showing the directional shift and relative magnitude of the shift, when compared with Sentinel-2, along with the corresponding histogram graphs and plots, are provided in [figures 38 through 43](#). The Sentinel-2 imagery had a control uncertainty of about 8 m.

In the second external geometric location accuracy procedure, a Pléiades Neo image over Sioux Falls, S. Dak., was compared to previously collected GCPs accurate to a 3-centimeter 90-percent circular error value. For this analysis, 27 to 66 GCPs over Sioux Falls, S. Dak., were manually measured on the Pléiades Neo panchromatic; three-band red, green, and blue (RGB); and three-band near-infrared, red edge, and deep blue (coastal aerosol; NED) bands, for nonorthorectified and orthorectified images, using the QGIS software (formerly known as Quantum Geographic Information System software). The horizontal coordinates derived from the image were compared to the known horizontal coordinates of the GCPs. Error statistics for each of the panchromatic, RGB, and NED bands for nonorthorectified and orthorectified images are listed in [tables 7 through 11](#). Geometric error maps showing the directional shift and relative magnitude of the shift, when compared with GCPs, are provided in [figures 44 through 53](#). The National Standard for Spatial Data Accuracy metric, which is a 95-percent circular error value, is 3.4 to 8.8 m. The 95-percent circular error value, which is denoted in [tables 7 through 11](#) as CE95, is 2.2 to 7.2 m. Refer to [appendix 1](#) for a more detailed explanation of the second geometric location accuracy procedure. We understand that Airbus does not use ground registration yet but plans to enhance the geolocation accuracy of the PRIMARY, PROJECTED, and ORTHO products soon. This will be available by the end of the year.

Table 5. Geometric error relative to Sentinel-2.

[ID, identifier; STD, standard deviation; RMSE, root mean square error; NIR, near infrared; m, meter]

Scene ID	Mean error (easting)	Mean error (northing)	STD (easting)	STD (northing)	RMSE (easting)	RMSE (northing)
PNEO4_202205121724235_MS-FS_SEN (Sioux Falls, South Dakota)—NIR	−0.702 pixel (−7.015 m)	0.385 pixel (3.846 m)	0.241 pixel (2.414 m)	0.239 pixel (2.386 m)	0.742 pixel (7.418 m)	0.453 pixel (4.525 m)
PNEO3_202110201751341_MS-FS_SEN (Fort Lupton, Colorado)—NIR	0.404 pixel (4.041 m)	0.056 pixel (0.560 m)	0.344 pixel (3.437 m)	0.162 pixel (1.624 m)	0.530 pixel (5.302 m)	0.172 pixel (1.717 m)

Table 6. Geometric error relative to Sentinel-2 (orthorectified).

[ID, identifier; STD, standard deviation; RMSE, root mean square error; NIR, near infrared; m, meter]

Scene ID	Mean error (easting)	Mean error (northing)	STD (easting)	STD (northing)	RMSE (easting)	RMSE (northing)
PNEO3_202203310331286_MS-FS_ORT (Baotou, Inner Mongolia, China)—NIR	−0.234 pixel (−2.341 m)	0.237 pixel (2.371 m)	0.086 pixel (0.864 m)	0.066 pixel (0.659 m)	0.250 pixel (2.495 m)	0.246 pixel (2.461 m)
PNEO4_202205121724235_MS-FS_ORT (Sioux Falls, South Dakota)—NIR	−0.574 pixel (−5.739 m)	0.095 pixel (0.951 m)	0.123 pixel (1.226 m)	0.137 pixel (1.365 m)	0.587 pixel (5.869 m)	0.166 pixel (1.663 m)
PNEO3_202110201751340_MS-FS_ORT (Fort Lupton, Colorado)—NIR	−0.393 pixel (−3.916 m)	0.286 pixel (2.856 m)	0.070 pixel (0.703 m)	0.057 pixel (0.573 m)	0.398 pixel (3.979 m)	0.291 pixel (2.913 m)

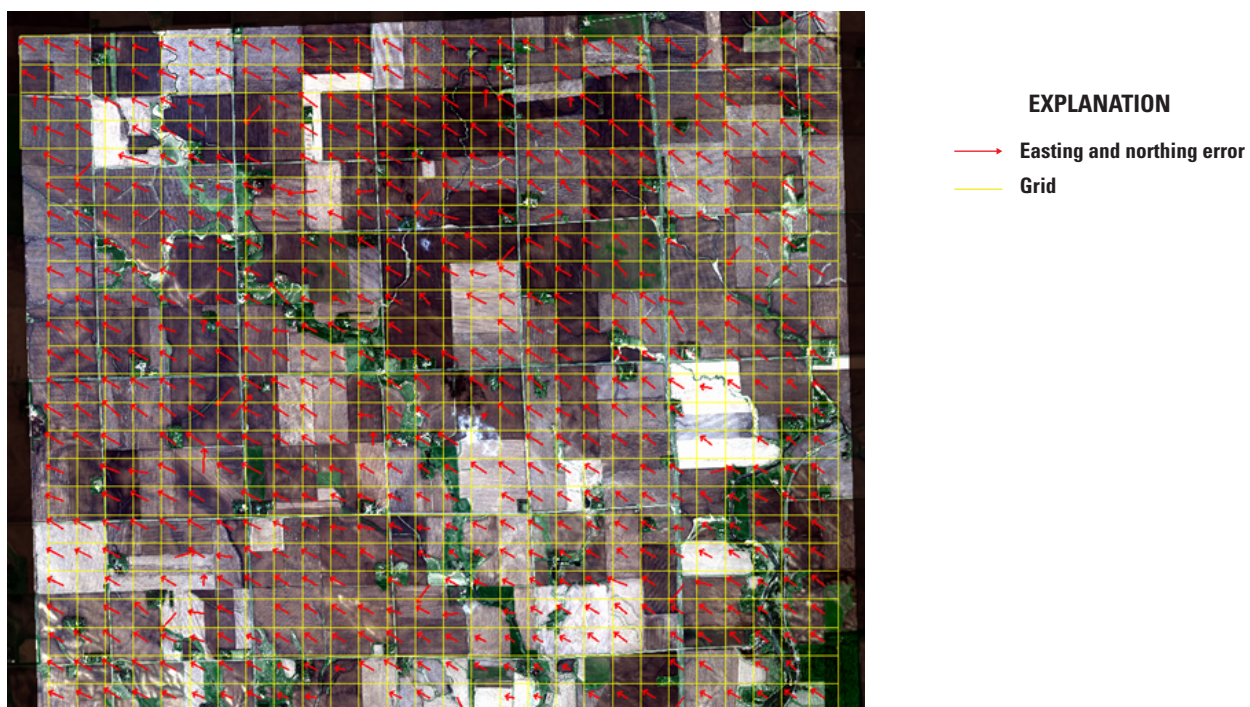


Figure 38. Relative geometric error comparison for Sentinel-2 and Pléiades Neo for the near-infrared band, Sioux Falls, South Dakota.

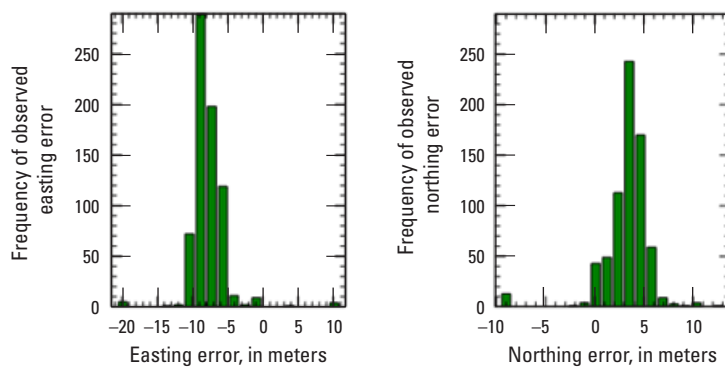


Figure 39. Relative geometric easting and northing error histogram comparison for Sentinel-2 and Pléiades Neo for the near-infrared band, Sioux Falls, South Dakota.

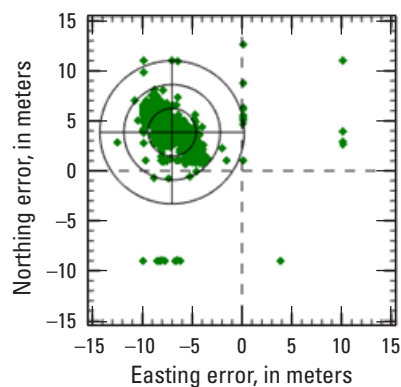


Figure 40. Relative geometric easting and northing error plot comparison for Sentinel-2 and Pléiades Neo for the near-infrared band, Sioux Falls, South Dakota.



Figure 41. Relative geometric error comparison for Sentinel-2 and Pléiades Neo for the near-infrared band, Fort Lupton, Colorado.

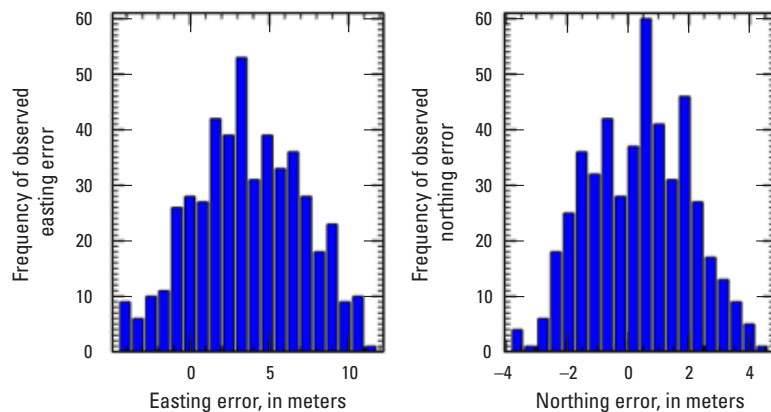


Figure 42. Relative geometric easting and northing error histogram comparison for Sentinel-2 and Pléiades Neo for the near-infrared band, Fort Lupton, Colorado.

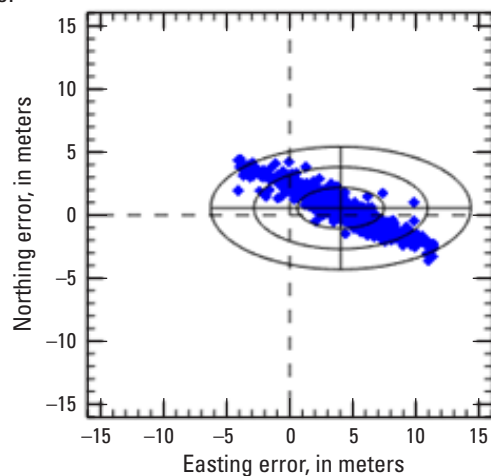


Figure 43. Relative geometric easting and northing error plot comparison for Sentinel-2 and Pléiades Neo for the near-infrared band, Fort Lupton, Colorado.

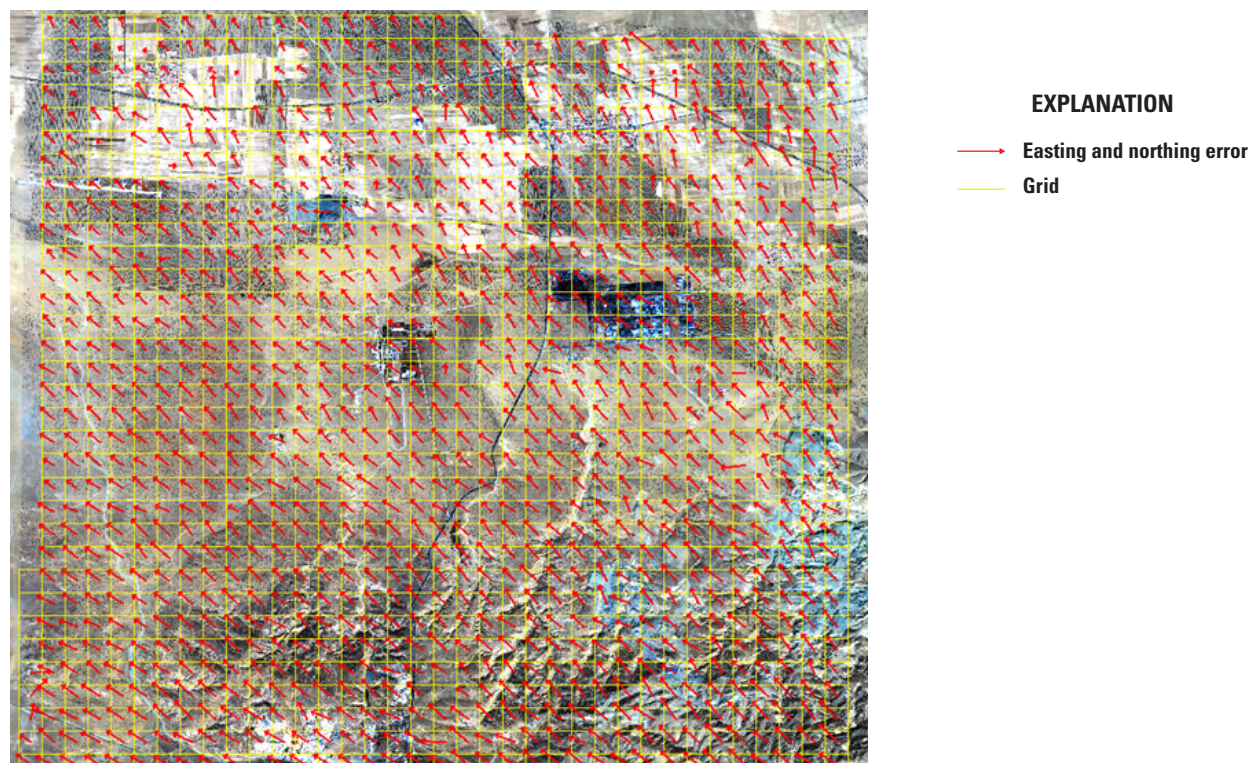


Figure 44. Relative geometric error comparison for Sentinel-2 and Pléiades Neo orthorectified image for the near-infrared band, Baotou, Inner Mongolia, China.

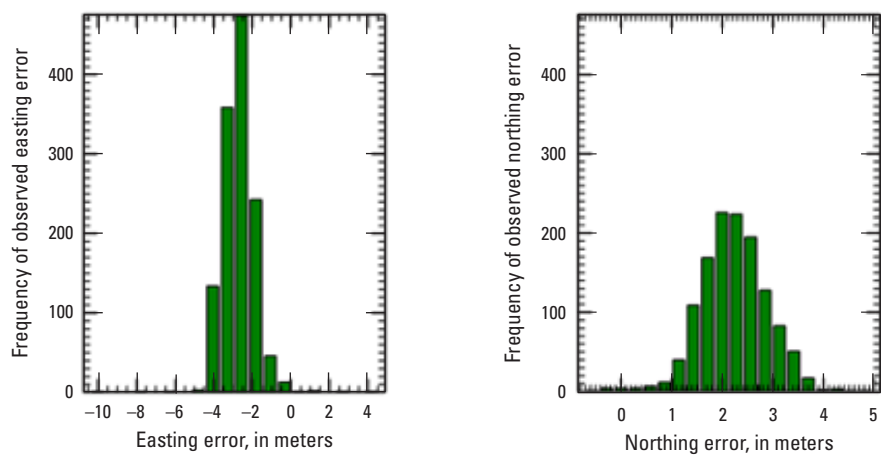


Figure 45. Relative geometric easting and northing error histogram comparison for Sentinel-2 and Pléiades Neo orthorectified image for the near-infrared band, Baotou, Inner Mongolia, China.

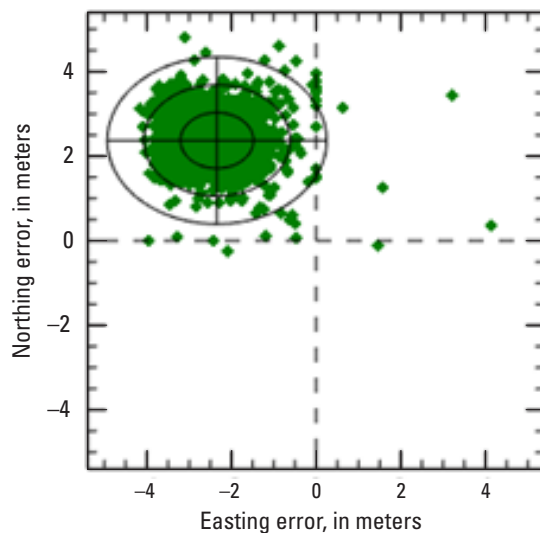


Figure 46. Relative geometric easting and northing error plot comparison for Sentinel-2 and Pléiades Neo orthorectified image for the near-infrared band, Baotou, Inner Mongolia, China.



Figure 47. Relative geometric error comparison for Sentinel-2 and Pléiades Neo orthorectified image for the near-infrared band, Fort Lupton, Colorado.

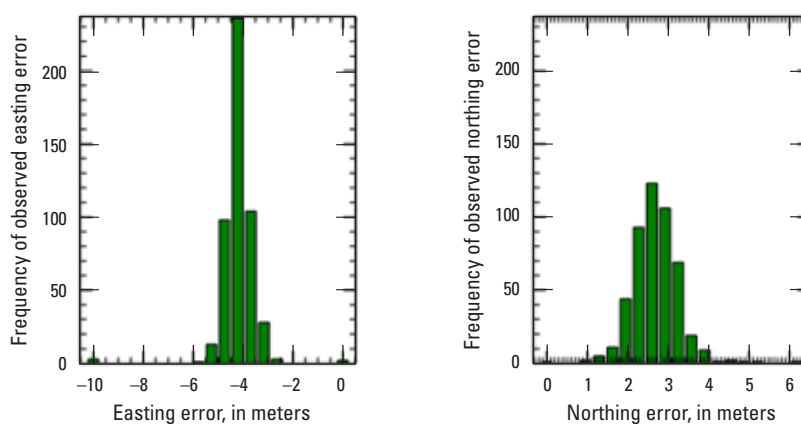


Figure 48. Relative geometric easting and northing error histogram comparison for Sentinel-2 and Pléiades Neo orthorectified image for the near-infrared band, Fort Lupton, Colorado.

Table 7. Geometric error of Pléiades Neo-4 primary panchromatic bands relative to ground-surveyed control points.

[ID, identifier; STD, standard deviation; RMSE, root mean square error; NSSDA, National Standard for Spatial Data Accuracy; %, percent; CE95, 95-percent circular error; GCP, ground control point; m, meter; ~, about]

Scene ID	Mean error (easting)	Mean error (northing)	STD (easting)	STD (northing)	RMSE (easting)	RMSE (northing)	NSSDA (95%)	CE95
Basic (28 GCPs) 202203261720599_PAN_SEN_ PWOI_000035190_2_1_F_1_P (Sioux Falls, South Dakota)	−3.8 m (~12.7 pixels)	−0.7 m (~2.3 pixels)	1.3 m (~4.3 pixels)	1.0 m (~3.3 pixels)	4.0 m (~13.3 pixels)	1.2 m (~4.0 pixels)	7.3 m (~24.3 pixels)	5.5 m (~18.3 pixels)
Basic (51 GCPs) 202203261721127_PAN_SEN_ PWOI_000035190_3_1_F_1_P (Sioux Falls, South Dakota)	−1.6 m (~5.3 pixels)	−1.0 m (~3.3 pixels)	0.2 m (~0.7 pixel)	0.4 m (~1.3 pixels)	1.6 m (~5.3 pixels)	1.1 m (~3.7 pixels)	3.4 m (~11.3 pixels)	2.2 m (~7.3 pixels)
Basic (64 GCPs) 202204161724354_PAN_SEN_ PWOI_000035190_1_1_F_1_P (Sioux Falls, South Dakota)	−1.3 m (~4.3 pixels)	−1.9 m (~6.3 pixels)	0.2 m (~0.7 pixel)	0.7 m (~2.3 pixels)	1.4 m (~4.7 pixels)	2.1 m (~7.0 pixels)	4.3 m (~14.4 pixels)	3.1 m (~10.3 pixels)

Table 8. Geometric error of Pléiades Neo-4 primary red, green, and blue bands relative to ground-surveyed control points.

[ID, identifier; STD, standard deviation; RMSE, root mean square error; NSSDA, National Standard for Spatial Data Accuracy; %, percent; CE95, 95-percent circular error; GCP, ground control point; m, meter; ~, about]

Scene ID	Mean error (easting)	Mean error (northing)	STD (easting)	STD (northing)	RMSE (easting)	RMSE (northing)	NSSDA (95%)	CE95
Basic (27 GCPs) 202203261720599_ MS-FS_SEN_PWOI_ 000035190_2_1_F_1_RGB (Sioux Falls, South Dakota)	−2.2 m (~1.8 pixels)	−2.3 m (~1.9 pixels)	1.3 (~1.1 pixels)	1.1 m (~0.9 pixel)	2.5 m (~2.1 pixels)	2.5 m (~2.1 pixels)	6.2 m (~5.2 pixels)	4.5 m (~3.8 pixels)
Basic (49 GCPs) 202203261721127_MS-FS_ SEN_PWOI_000035190_ 3_1_F_1_RGB (Sioux Falls, South Dakota)	0.0 m (~0.0 pixels)	−2.6 m (~2.2 pixels)	0.5 m (~0.4 pixel)	0.5 m (~0.4 pixel)	0.5 m (~0.4 pixel)	2.7 m (~2.3 pixels)	4.7 m (~3.9 pixels)	3.4 m (~2.8 pixels)
Basic (65 GCPs) 202204161724354_MS-FS_ SEN_PWOI_000035190_ 1_1_F_1_RGB (Sioux Falls, South Dakota)	0.3 m (~0.3 pixel)	−3.4 m (~2.8 pixels)	0.5 m (~0.4 pixel)	0.7 m (~0.6 pixel)	0.5 m (~0.4 pixel)	3.5 m (~2.9 pixels)	6.1 m (~5.1 pixels)	4.6 m (~3.8 pixels)

Table 9. Geometric error of Pléiades Neo-4 orthorectified panchromatic bands relative to ground-surveyed control points.

[ID, identifier; STD, standard deviation; RMSE, root mean square error; NSSDA, National Standard for Spatial Data Accuracy; %, percent; CE95, 95-percent circular error; GCP, ground control point; m, meter; ~, about]

Scene ID	Mean error (easting)	Mean error (northing)	STD (easting)	STD (northing)	RMSE (easting)	RMSE (northing)	NSSDA (95%)	CE95
Basic (28 GCPs) 202203261720599_PAN_ORT_ PWOI_000035193_3_1_F_1_P (Sioux Falls, South Dakota)	−4.3 m (~14.3 pixels)	−0.1 m (~0.3 pixel)	1.3 m (~4.3 pixels)	1.1 m (~3.7 pixels)	4.5 m (~15.0 pixels)	1.1 m (~3.7 pixels)	8.1 m (~27.0 pixels)	6.5 m (~21.7 pixels)
Basic (49 GCPs) 202203261721126_PAN_ORT_ PWOI_000035193_2_1_F_1_P (Sioux Falls, South Dakota)	−2.1 m (~7.0 pixels)	−0.7 m (~2.3 pixels)	0.4 m (~1.3 pixels)	0.6 m (~2.0 pixels)	2.2 m (~7.3 pixels)	0.9 m (~3.0 pixels)	4.0 m (~13.3 pixels)	2.9 m (~9.7 pixels)
Basic (66 GCPs) 202204161724353_PAN_ORT_ PWOI_000035193_1_1_F_1_P (Sioux Falls, South Dakota)	−2.0 m (~6.7 pixels)	−1.2 m (~4.0 pixels)	0.3 m (~1.0 pixel)	0.7 m (~2.3 pixels)	2.0 m (~6.7 pixels)	1.4 m (~4.7 pixels)	4.2 m (~14.0 pixels)	2.9 m (~9.7 pixels)

Table 10. Geometric error of Pléiades Neo-4 orthorectified red, green, and blue bands relative to ground-surveyed control points.

[ID, identifier; STD, standard deviation; RMSE, root mean square error; NSSDA, National Standard for Spatial Data Accuracy; %, percent; CE95, 95-percent circular error; GCP, ground control point; m, meter; ~, about]

Scene ID	Mean error (easting)	Mean error (northing)	STD (easting)	STD (northing)	RMSE (easting)	RMSE (northing)	NSSDA (95%)	CE95
Basic (28 GCPs) 2203261720599_MS-FS_ORT_ PWOI_000035193_3_1_F_1_RGB (Sioux Falls, South Dakota)	−4.7 m (~3.9 pixels)	0.4 m (~0.3 pixel)	1.4 m (~1.2 pixels)	1.3 m (~1.1 pixels)	4.8 m (~4.0 pixels)	1.4 m (~1.2 pixels)	8.7 m (~7.3 pixels)	7.2 m (~6.0 pixels)
Basic (50 GCPs) 02203261721126_MS-FS_ORT_ PWOI_000035193_2_1_F_1_RGB (Sioux Falls, South Dakota)	−2.5 m (~2.1 pixels)	0.0 m (~0.0 pixels)	0.7 m (~0.6 pixel)	0.6 m (~0.5 pixel)	2.6 m (~2.2 pixels)	0.6 m (~0.5 pixel)	4.6 m (~3.8 pixels)	3.5 m (~2.9 pixels)
Basic (65 GCPs) 02204161724353_MS-FS_ORT_ PWOI_000035193_1_1_F_1_RGB (Sioux Falls, South Dakota)	−2.3 m (~1.9 pixels)	−0.6 m (~0.5 pixel)	0.6 m (~0.5 pixel)	0.9 m (~0.8 pixel)	2.4 m (~2.0 pixels)	1.1 m (~0.9 pixel)	4.5 m (~3.8 pixels)	3.4 m (~2.8 pixels)

Table 11. Geometric error of Pléiades Neo-4 orthorectified near-infrared, red edge, and deep blue (coastal aerosol) bands relative to ground-surveyed control points.

[ID, identifier; STD, standard deviation; RMSE, root mean square error; NSSDA, National Standard for Spatial Data Accuracy; %, percent; CE95, 95-percent circular error; GCP, ground control point; m, meter; ~, about]

Scene ID	Mean error (easting)	Mean error (northing)	STD (easting)	STD (northing)	RMSE (easting)	RMSE (northing)	NSSDA (95%)	CE95
Basic (27 GCPs) 202203261720599_ MS-FS_ORT_ PWOI_000035193_ 3_1_F_1_NED (Sioux Falls, South Dakota)	−4.7 m (~3.9 pixels)	0.4 m (~0.3 pixel)	1.4 m (~1.2 pixels)	1.4 m (~1.2 pixels)	4.8 m (~4.0 pixels)	1.4 m (~1.2 pixels)	8.8 m (~7.3 pixels)	7.0 m (~5.8 pixels)
Basic (49 GCPs) 202203261721126_ MS-FS_ORT_ PWOI_000035193_ 2_1_F_1_NED (Sioux Falls, South Dakota)	−2.5 m (~2.1 pixels)	0.0 m (~0.0 pixels)	0.7 m (~0.6 pixel)	0.7 m (~0.6 pixel)	2.6 m (~2.2 pixels)	0.7 m (~0.6 pixel)	4.6 m (~3.8 pixels)	3.9 m (~3.3 pixels)
Basic (64 GCPs) 202204161724353_ MS-FS_ORT_ PWOI_000035193_ 1_1_F_1_NED (Sioux Falls, South Dakota)	−2.3 m (~1.9 pixels)	−0.6 m (~0.5 pixel)	0.5 m (~0.4 pixel)	0.9 m (~0.8 pixel)	2.4 m (~2.0 pixels)	1.0 m (~0.8 pixel)	4.4 m (~3.7 pixels)	3.3 m (~2.8 pixels)

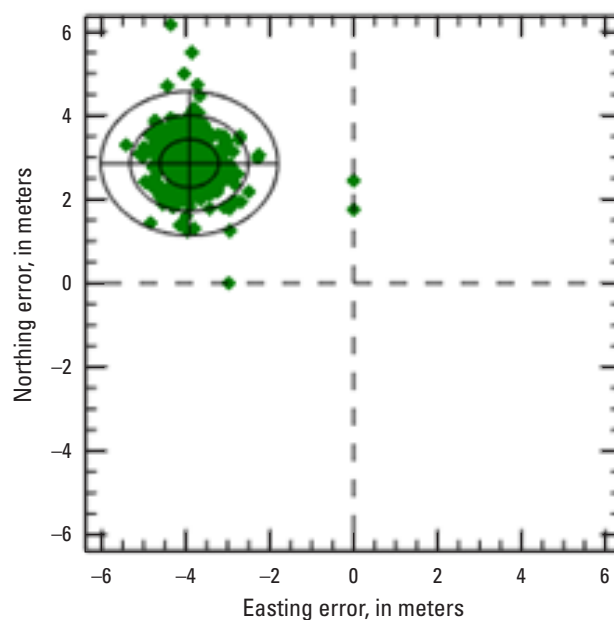


Figure 49. Relative geometric easting and northing error plot comparison for Sentinel-2 and Pléiades Neo orthorectified image for the near-infrared band, Fort Lupton, Colorado.

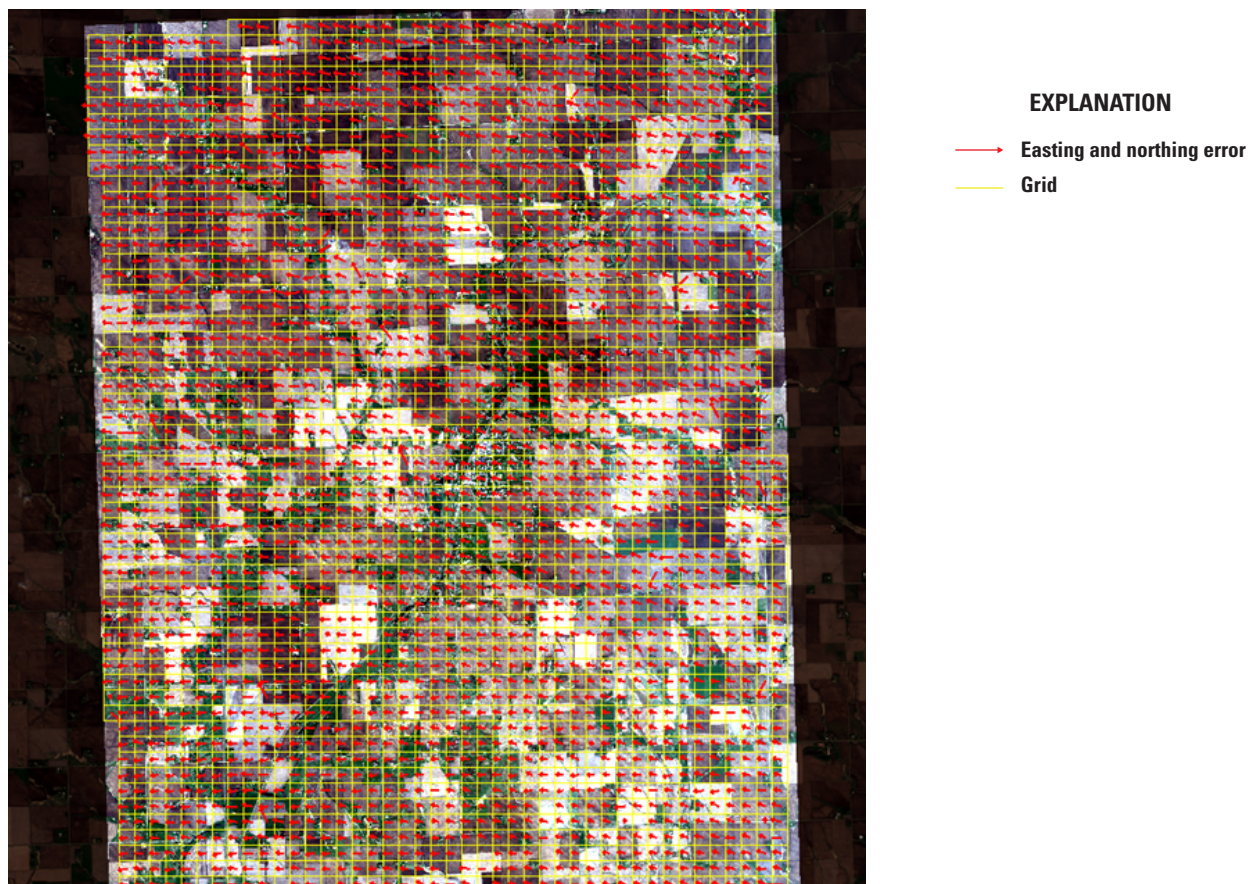


Figure 50. Relative geometric error comparison for Sentinel-2 and Pléiades Neo orthorectified image for the near-infrared band, Sioux Falls, South Dakota.

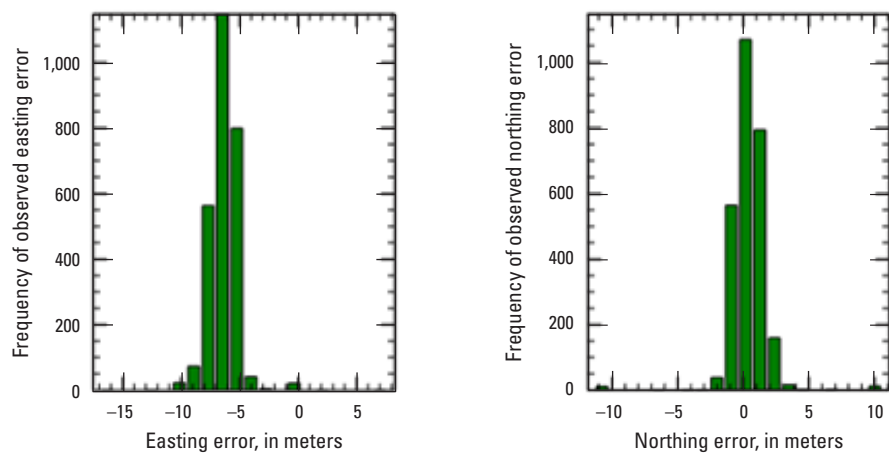


Figure 51. Relative geometric easting and northing error histogram comparison for Sentinel-2 and Pléiades Neo orthorectified image for the near-infrared band, Sioux Falls, South Dakota.

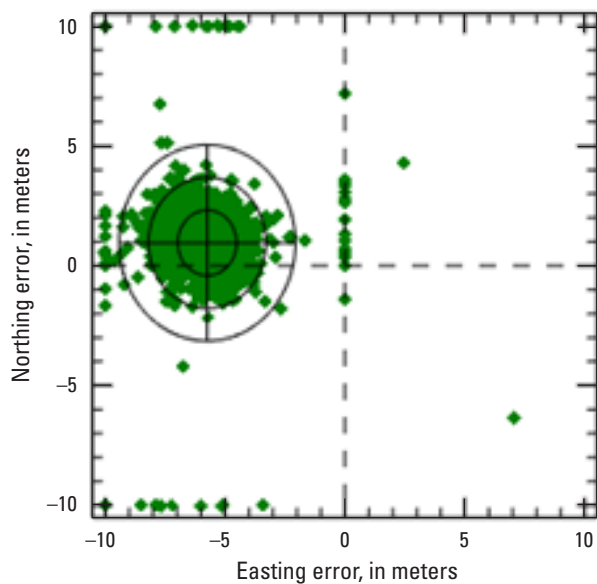


Figure 52. Relative geometric easting and northing error plot comparison for Sentinel-2 and Pléiades Neo orthorectified image for the near-infrared band, Sioux Falls, South Dakota.

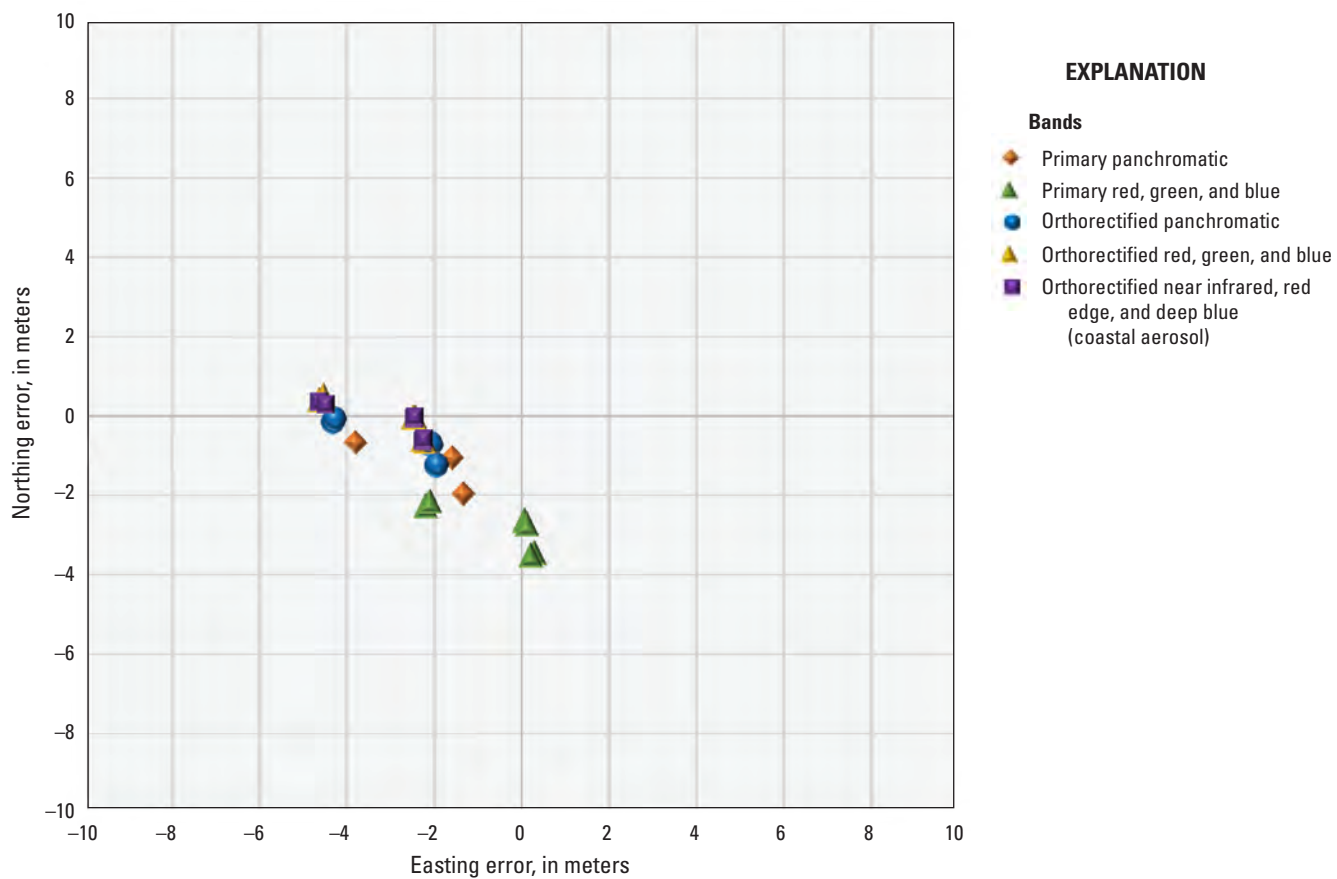


Figure 53. Pléiades Neo horizontal geolocation accuracy error plot (mean accuracy) for primary panchromatic and red, green, and blue and orthorectified panchromatic; red, green, and blue; and near-infrared, red edge, and deep blue (coastal aerosol) band scenes.

Radiometric Performance

Radiometric performance was evaluated using linear regression. For this analysis, cloud-free regions of interest were selected within a near-coincident Pléiades Neo and Sentinel-2 scene pair over a site in Fort Lupton, Colo. (Pléiades Neo scene identifier PNEO3_202110201751341_MS-FS_SEN, Sentinel-2B scene identifier L1C_T13TEE_A024148_20211020T174348). Once the relative georeferencing error between Sentinel-2 and Pléiades Neo has been corrected, Top of Atmosphere reflectance values from the two sensors are extracted. The scatterplots in figure 54 show the reference sensor data on the x-axis and the comparison sensor data on the y-axis. The linear regression, thus, represents Top of Atmosphere

reflectance relative to that of the reference sensor. Ideally, the slope should be near unity, and the offset should be near zero; for example, if the slope is greater than unity, that means the comparison sensor has a tendency to overestimate Top of Atmosphere reflectance compared to the reference sensor.

Top of Atmosphere reflectance comparison results for VNIR bands are listed in table 12. Pléiades Neo VNIR bands 3, 4, 5, and 7 were chosen because they each correlate well with a corresponding Sentinel-2 band. A VNIR band-to-band graphical comparison between the Pléiades Neo image over Fort Lupton, Colo., when compared with the corresponding Sentinel-2 band, is shown in figure 54. The band-to-band comparison for the Fort Lupton scene indicates good agreement between the two images.

Table 12. Top of Atmosphere reflectance comparison of Pléiades Neo images against Sentinel-2 images.

[ID, identifier; VNIR, visible and near infrared; NIR, near infrared; %, percent; *R*², coefficient of determination]

Scene IDs	Statistics	VNIR bands			
		Band 3—Blue	Band 4—Green	Band 5—Red	Band 7—NIR
Sentinel-2: L1C_T13TEE_A024148_20211020T174348;	Uncertainty (%)	3.33	4.74	5.12	5.12
Pléiades Neo: PNEO3_202110201751341_MS-FS_SEN (Fort Lupton, Colorado)	<i>R</i> ²	0.905	0.913	0.912	0.903
	Radical offset	−0.004	−0.013	−0.013	−0.022
	Radical slope	1.067	1.139	1.074	1.144

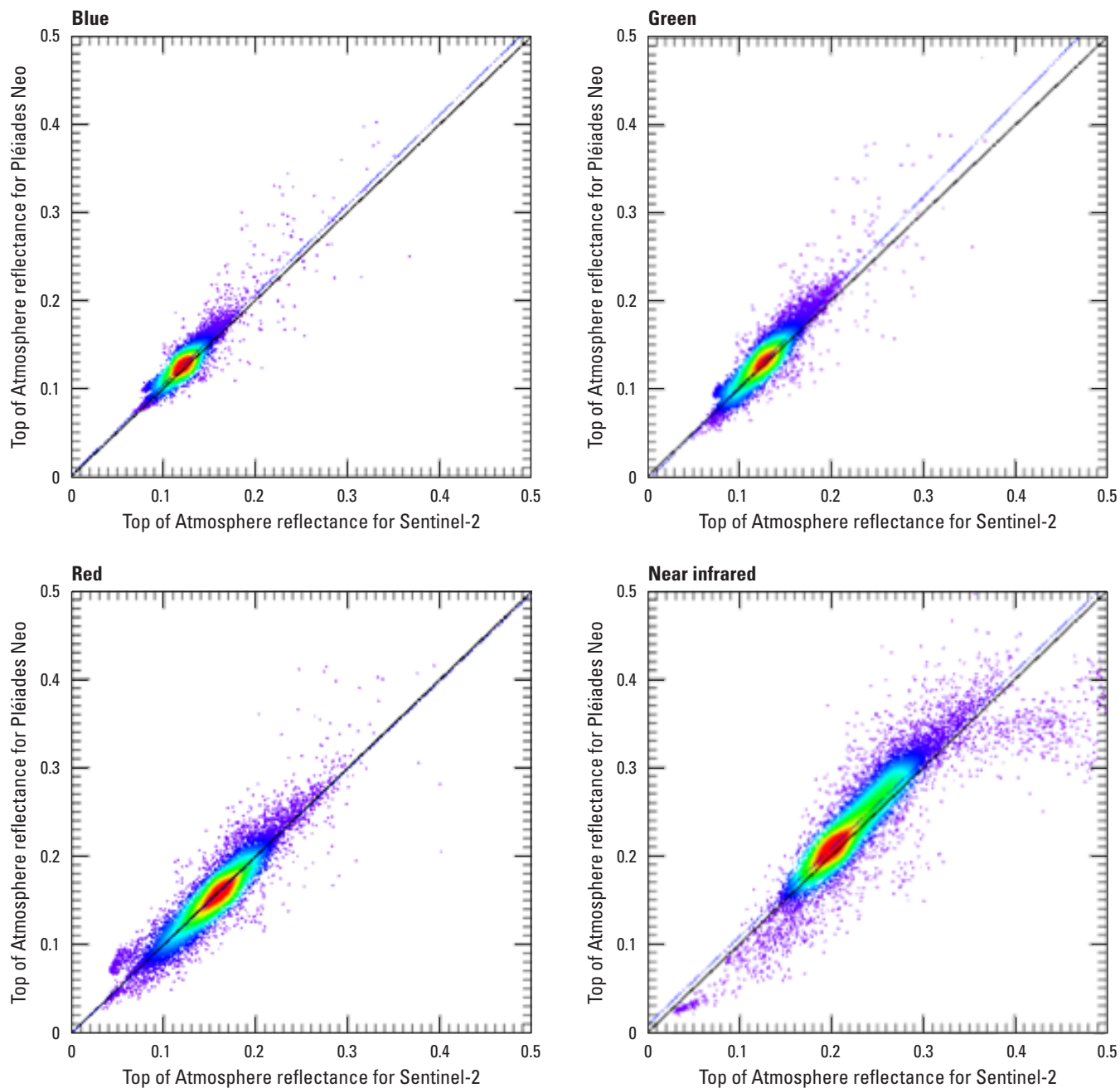


Figure 54. Top of Atmosphere reflectance comparison for Pléiades Neo and Sentinel-2 for blue, green, red, and near-infrared bands for Fort Lupton, Colorado, on October 20, 2021.

Spatial Performance

For this analysis, edge spread and line spread functions were calculated with resulting full width at half maximum and modulation transfer function at Nyquist frequency analysis outputs, as listed in table 13. The Pléiades Neo image used for the analysis is “IMG_PNEO3_202203310331286_PAN_SEN_

PWOI_000028089_2_1_F_1_P_R1C1.tif” for Baotou, Inner Mongolia, China (fig. 55), and includes the calibration site. The results for the orthorectified band are shown in figures 56 and 57. The raw edge transect with bounding box selected is shown in figure 56, and the edge spread function (upper) and line spread function and modulation transfer function (lower) are shown in figure 57A–D.

Table 13. Spatial performance of Pléiades Neo.

[RER, relative edge response; FWHM, full width at half maximum; MTF, modular transfer function; NIR, near infrared]

Spatial analysis	RER	FWHM	MTF at Nyquist
Band 1—Panchromatic	0.589	1.377 pixels	0.1648
Band 2—Coastal aerosol	0.762	1.002 pixels	0.3422
Band 3—Blue	0.733	1.054 pixels	0.3110
Band 4—Green	0.650	1.226 pixels	0.2231
Band 5—Red	0.716	1.087 pixels	0.2924
Band 6—Red edge	0.746	1.029 pixels	0.3251
Band 7—NIR	0.685	1.149 pixels	0.2597

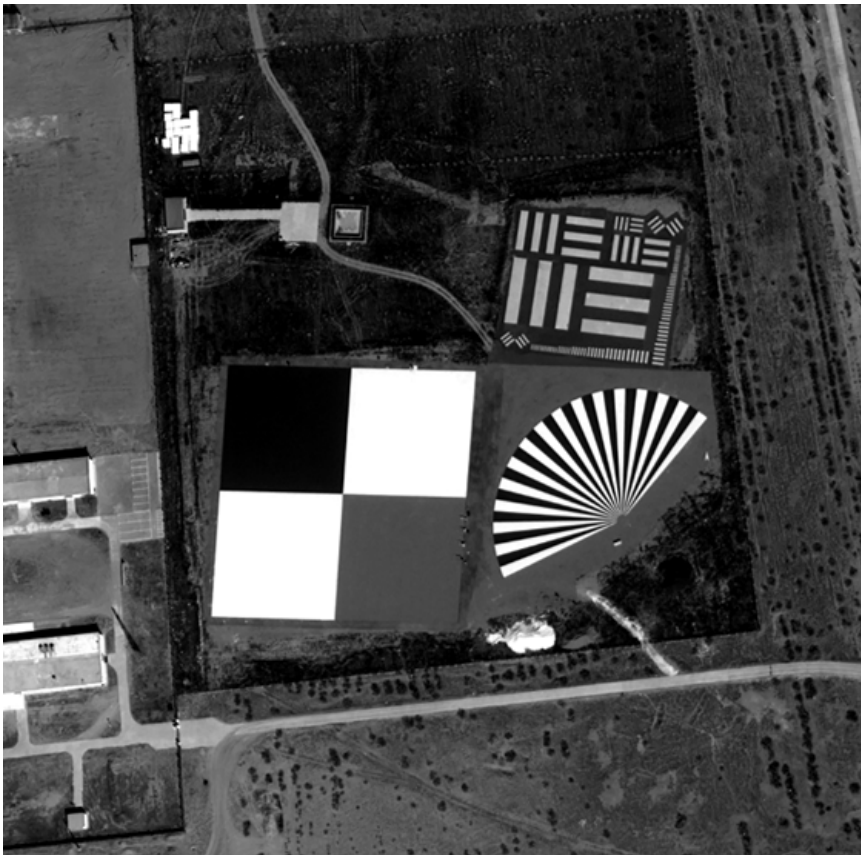


Figure 55. Pléiades Neo image of calibration site at Baotou, Inner Mongolia, China.

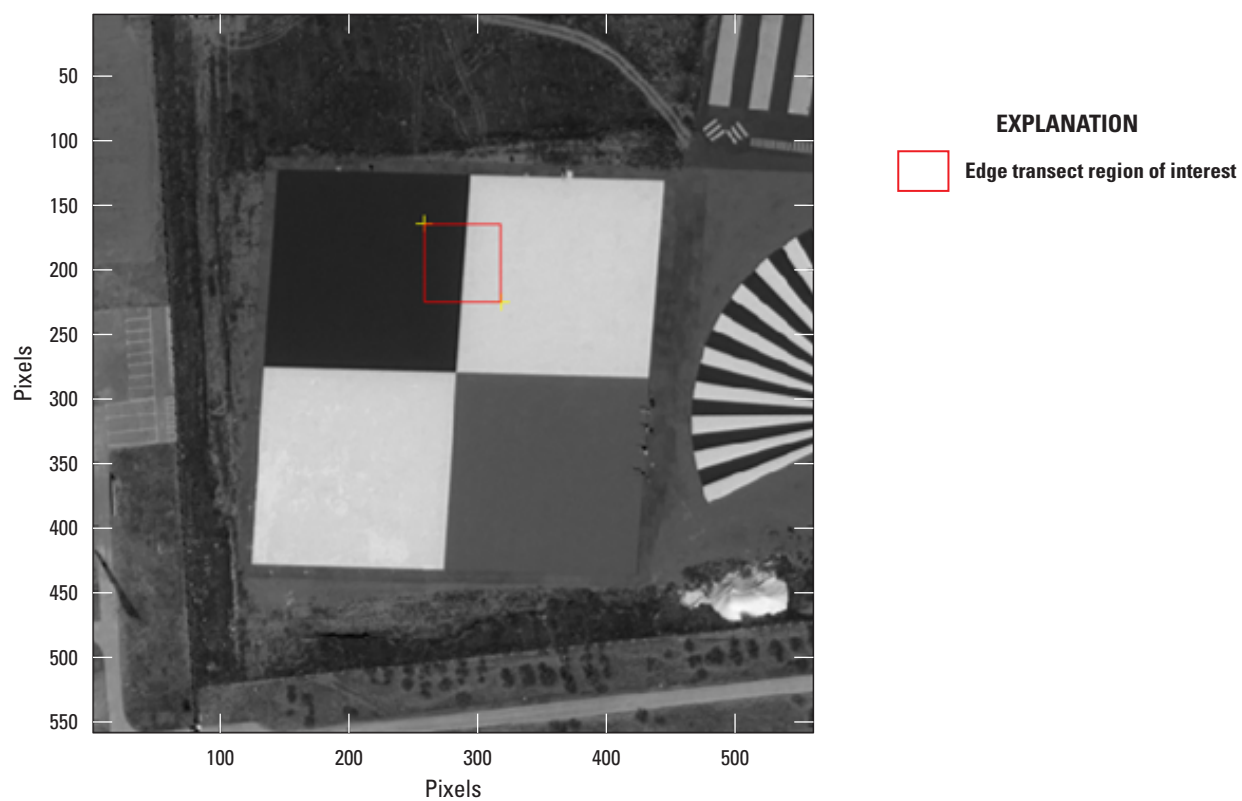
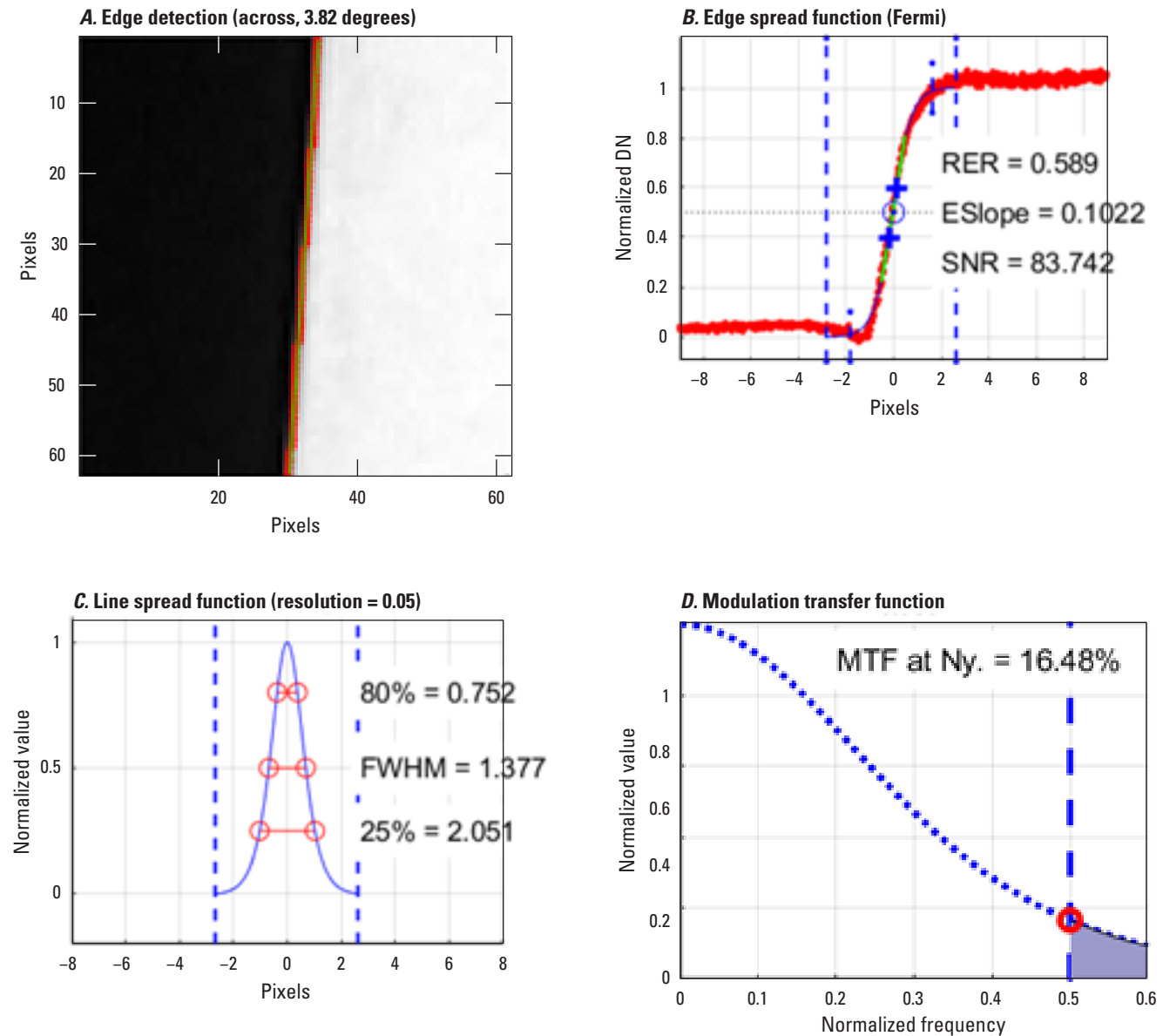


Figure 56. Band 1, panchromatic (orthorectified), raw edge transect selected within the region of interest at Baotou, Inner Mongolia, China.



EXPLANATION













- | | | |
|--|---|--|
|  Area that exceeds modulation transfer function at Nyquist—Images are subject to aliasing |  Beginning of edge and end of edge |  Limited region where slope is calculated—0.4 to 0.6 |
|  Extended region where slope is calculated—0.2 to 0.8 |  Line spread function plot |  Center pixel on edge spread function plot |
|  Excluded region of edge spread function |  Region of line spread function |  Point at which modulation transfer function at Nyquist occurs—0.5 normalized frequency |
|  Range of pixels where edge is present in the image |  25 percent, 50 percent, and 80 percent regions of line spread function plot | |
| |  Modulation transfer function plot | |

Figure 57. Band 1, panchromatic (orthorectified), (A) raw edge transect, (B) edge spread function, (C) line spread function, and (D) modulation transfer function at Baotou, Inner Mongolia, China. [DN, descending node; RER, relative edge response; ESlope, edge slope; SNR, signal to noise ratio; %, percent; FWHM, full width at half maximum; MTF, modulation transfer function; Ny., Nyquist]

Summary and Conclusions

This report summarizes the sensor performance of the Airbus Defence and Space Pléiades Neo system based on the U.S. Geological Survey Earth Resources Observation and Science Cal/Val Center of Excellence (ECCOE) system characterization process. In summary, we have determined that this sensor has an interior geometric performance in the range of 0.01 meter (m) (0.008 pixel) to -0.017 m (-0.014 pixel) in band-to-band registration; an exterior geometric performance in the range of -7.015 m (-0.702 pixel) to 3.846 m (0.385 pixel) offset in comparison to Sentinel-2 using ground control points of 2.2 to 7.2 m (95-percent circular error); a radiometric performance in the range of -0.070 (minimum) to -0.053 (maximum) in offset and 1.107 (minimum) to 1.202 (maximum) in slope; and a spatial performance in the range of 1.002 to 1.226 pixels at full width at half maximum with a modulation transfer function at a Nyquist frequency in the range of 0.22 to 0.34 (bands 2–7).

In conclusion, the team has completed an ECCOE standardized system characterization of the Pléiades Neo sensing system. Although the team followed characterization procedures that are standardized across the many sensors and sensing systems under evaluation, these procedures are customized to fit the individual sensor, as was done with Pléiades Neo. The team has acquired the data, defined proper testing methodologies, carried out comparative tests against specific references, recorded measurements, completed data analyses, and quantified sensor performance accordingly. The team also endeavored to retain all data, measurements, and methods. This is key to ensure that all data and measurements are archived and accessible and that the performance results are reproducible.

The ECCOE project and associated Joint Agency Commercial Imagery Evaluation partners are always interested in reviewing sensor and remote sensing application assessments and would like to collaborate and discuss information on similar data and product assessments and reviews. If you would like to discuss system characterization with the U.S. Geological Survey ECCOE and (or) the Joint Agency Commercial Imagery Evaluation team, please email us at eccoe@usgs.gov.

Selected References

- Ramaseri Chandra, S.N., Christopherson, J.B., Casey, K., Oeding, J., Ranjitkar, B., and Rusten, T., 2022, Land remote sensing satellites online compendium: U.S. Geological Survey digital data, accessed November 2022, at <https://calval.cr.usgs.gov/apps/compendium>.
- Satellite Imaging Corporation, 2022, Pleiades Neo satellite constellation (30cm): Satellite Imaging Corporation web page, accessed November 2022 at <https://www.satimagingcorp.com/satellite-sensors/pleiades-Neo/>.
- U.S. Geological Survey, 2022a, EROS CalVal Center of Excellence (ECCOE)—JACIE: U.S. Geological Survey web page, accessed November 2022 at https://www.usgs.gov/calval/jacie?qt-science_support_page_related_con=3#qt-science_support_page_related_con.
- U.S. Geological Survey, 2022b, Landsat missions—Glossary and acronyms: U.S. Geological Survey web page, accessed November 2022 at <https://www.usgs.gov/core-science-systems/nli/landsat/glossary-and-acronyms>.

Appendix 1. Explanation of Ground Control Points Method and Metadata

For this analysis, ground control points (GCPs) over Sioux Falls, South Dakota (43.52° N., -96.64° E.), were manually measured using the QGIS software (formerly known as Quantum Geographic Information System software) where visible on three image collections from the Pléiades Neo-4 satellite. The GCPs were collected via Global Positioning System hand-held devices and are accurate to a 3-centimeter 90-percent circular error value. Each collected image was processed four ways:

1. primary geometry (perspective) with basic (detector equalization) radiometric processing,
2. primary geometry with reflectance (atmospherically corrected) radiometric processing,
3. orthorectified geometry with basic radiometric processing, and
4. orthorectified geometry with reflectance radiometric processing.

For each type of processing, spectral bands were stored in three GeoTIFF files—the first containing the 0.3-meter (m; nadir) ground sample distance (GSD) panchromatic band; the second containing the 1.2-m (nadir) GSD red, green, and blue (RGB) bands; and the third containing the 1.2-m GSD near infrared, red edge, and deep blue (coastal aerosol; NED) bands.

Geolocation for primary imagery was based on image pixel-to-ground elevation perspective projections using rational polynomial coefficient data unique to each image and stored in an Extensible Markup Language (more commonly known as XML) file delivered with the imagery product. Each image pixel corresponding to a GCP was measured using QGIS. Then, using Python code and the rational polynomial coefficient data, that pixel location was projected down to the ellipsoid height of that GCP to obtain its measured horizontal geodetic (latitude and longitude) coordinates based on the World Geodetic System of 1984 datum. Because each pair of RGB and NED images shares the same rational polynomial coefficient Extensible Markup Language file and the RGB and NED image products were visually assessed to be coregistered, only the RGB primary images were measured for geometric accuracy.

Geolocation for the orthorectified images was based on direct measurements of GCP easting and northing coordinates in QGIS using the World Geodetic System of 1984 Universal Transverse Mercator Zone 14 north projection (European Petroleum Survey Group code EPSG:32614) information stored in the GeoTIFFs. Each set of horizontal coordinates derived from an image pixel was compared to the known set of horizontal coordinates of the corresponding GCP to determine the horizontal errors for that point.

For more information about this publication, contact:

Director, USGS Earth Resources Observation and Science Center
47914 252nd Street
Sioux Falls, SD 57198
605-594-6151

For additional information, visit: <https://www.usgs.gov/centers/eros>

Publishing support provided by the
Rolla Publishing Service Center

